European Journal of Medicinal Chemistry 118 (2016) 276–289

Contents lists available at ScienceDirect

European Journal of Medicinal Chemistry

journal homepage: http://www.elsevier.com/locate/ejmech

Research paper

Design, synthesis, anti-tumor activity, and molecular modeling of quinazoline and pyrido[2,3-*d*]pyrimidine derivatives targeting epidermal growth factor receptor

Ju Hou [1], Shanhe Wan [1], Guangfa Wang, Tingting Zhang, Zhonghuang Li, Yuanxin Tian, Yonghuan Yu, Xiaoyun Wu**, Jiajie Zhang*

Guangdong Provincial Key Laboratory of New Drug Screening, School of Pharmaceutical Science, Southern Medical University, Guangzhou, 510515, PR China

ARTICLE INFO

Article history:
Received 26 December 2015
Received in revised form
22 March 2016
Accepted 8 April 2016
Available online 20 April 2016

Keywords:
EGFR inhibitor
Quinazoline and pyrido[2,3-*d*]pyrimidine derivatives
Antitumor
Molecular docking
Molecular dynamics simulation

ABSTRACT

Three series of novel quinazoline and pyrido[2,3-*d*]pyrimidine derivatives were designed, synthesized and evaluated for their ability to inhibit EGFR tyrosine kinase and a panel of five human cancer cell lines (MCF-7, A549, BT-474, SK-BR-3, and MDA-MB-231). Bioassay results indicated that five of these prepared compounds (**12c**–**12e** and **13c**–**13d**) exhibited remarkably higher inhibitory activities against EGFR and SK-BR-3 cell line. Compounds **12c** and **12e** displayed the most potent EGFR inhibitory activity (IC_{50} = 2.97 nM and 3.58 nM, respectively) and good anti-proliferative effect against SK-BR-3 cell with the IC_{50} values of 3.10 μM and 5.87 μM, respectively. Furthermore, molecular docking and molecular dynamics simulation studies verified that compound **12c** and **12e** shared similar binding pattern with gefitinib in the binding pocket of EGFR. MM-GBSA binding free energy revealed that the compound **12c** and **12e** have almost the same inhibitory activity against EGFR as gefitinib, and that the dominating effect of van der Waals interactions drives the binding process.

1. Introduction

Epidermal growth factor receptor (EGFR) belongs to the ErbB family of receptor tyrosine kinases. This family includes homologous receptors: the epidermal growth factor receptor (ErbB1/EGFr/HER1), ErbB2 (HER2/neu), ErbB3 (HER3), and ErbB4 (HER4). These receptors are composed of an extracellular ligand-binding domain, a transmembrane lipophilic segment, and an intracellular protein tyrosine kinase domain with a regulatory carboxyl terminal segment [1]. When ligands bind to these domains, receptor dimerization and autophosphorylation of intracellular tyrosine kinase domains occur. Autophosphorylation activating the downstream signaling pathways leads to diverse effects including cell proliferation, survival, adhesion, migration, and differentiation [2,3]. Previous research has demonstrated that EGFR is a putative oncogene and has been found in many human solid malignancies including non-small-cell lung cancer, ovarian cancer, breast cancer, etc [4]. Therefore, EGFR tyrosine kinase represents an attractive target for the treatment of many human cancers.

Quinazoline derivatives have long been recognized as an important scaffold for designing anti-EGFR agents [5,6]. The clinical success of selective kinase inhibitors, such as gefitinib [7,8], lapatinib [9], erlotinib [10], and canertinib [11,12] (Fig. 1), as therapeutic agents for several human cancers has prompted substantial interest in the further development and clinical testing of such inhibitors for a wide variety of malignancies. On the other hand, pyrido[2,3-d]pyrimidine derivatives also can be interacted with ATP-binding site of EGFR catalytic domain to inhibit EGFR [13,14]. Compound **A-1** (Fig. 1) belongs to the pyrido[2,3-d]pyrimidines, which showed nanomolarly potent EGFR inhibitory activity [14]. Quinazoline and pyrido[2,3-*d*]pyrimidine derivatives displayed favorable inhibitory activities against EGFR spured us on to greater efforts to develop novel and highly potent EGFR inhibitors.

Based on the crystal structure of EGFR complexed with gefitinib, we undertook the design of quinazoline and pyrido[2,3-*d*]pyrimidine derivatives having different substituents at C-2, C-4, and C-6 positions. To increase the hydrogen bond interactions with hinge region of the kinase, an amino group was introduced to C-2 position of the quinazoline core. In order to extend into the solvent region

* Corresponding author.
** Corresponding author.
E-mail addresses: xywugz@163.com (X. Wu), zhangjj@smu.edu.cn (J. Zhang).
[1] These authors contributed equally to this work.

http://dx.doi.org/10.1016/j.ejmech.2016.04.026
0223-5234/

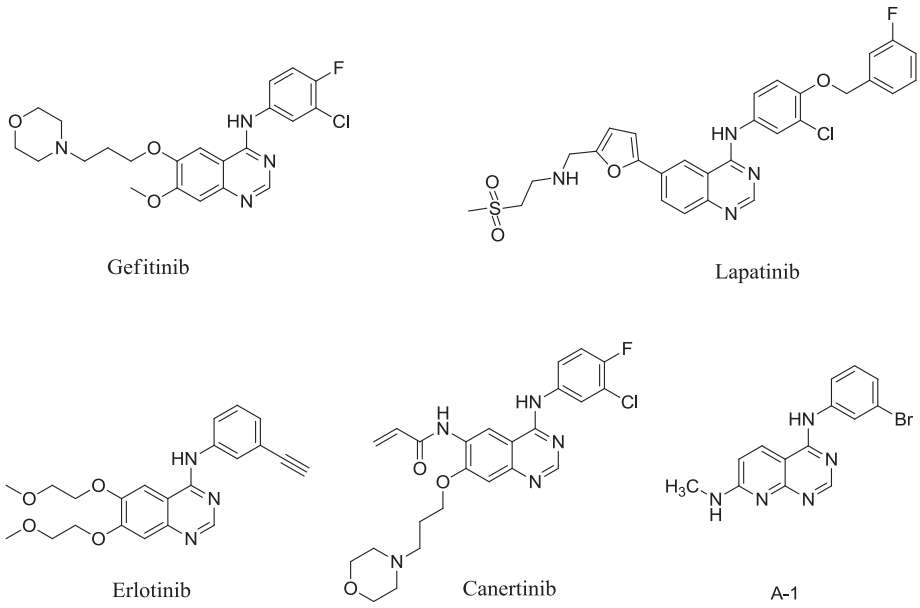

Fig. 1. Structure of EGFR small molecule inhibitors.

surrounding the kinase hinge segment, introduction of the polar N-substituted pyrazole fragments at the C-6 position of quinazoline and pyrido[2,3-*d*]pyrimidine scaffolds was investigated. Different kinds of aryl fragments connected to quinazoline and pyrido[2,3-*d*] pyrimidine nucleus through O-linker or N-linker at C-4 position were investigated to increase hydrophobic interactions with the hydrophobic pocket, which are crucial for EGFR inhibitory activity. Herein, we would like to report the synthesis and biological evaluation of these new series compounds for the first time.

2. Results and discussion

2.1. Chemistry

The synthetic strategy to prepare the target compounds is illustrated in Schemes 1–3. The bromination of the starting material **1** led to 2-amino-5-bromonicotinic acid (**2**), followed by cycilzation with formamide to give compound **3** [15], which was chloride with thionyl chloride using DMF as catalyst to afford **4**. The chlorine in the 4-position of intermediate **4** could be displaced with a variety of benzylamines to achieve intermediates **5a**–**5d**. Introduction of the pyrazole fragment at the C-6 position of **5a**–**5d** by conventional Suzuki coupling with the corresponding pyrazole boronic esters to obtain desired compounds **7a**–**7d** of series-**I**, or further deprotection of the Boc group of intermediate smoothly to give desired compound **6** of series-**I** [15].

Likewise, compounds **9** and **10**, which were prepared following the similar procedure described above for the preparation of **3** and **4**, respectively. Compound **10** was displaced with a variety of nucleophiles. The resulting intermediates **11a**–**11g** were converted to target compounds **12a**–**12f** and **13a**–**13d** of series-**II** by Suzuki coupling reaction as described in Scheme 2.

The intermediate **16** was produced from **14** by the reaction with dicyandiamide followed by the cleavage of the amidino moiety of **15** [16], which was condensed with different reagents to give the desired products **17a**–**17b**. Final compounds **18** and **19a**–**19b** of series-**III** were similarly obtained of series-**I** as shown in Scheme 3.

The structures of all the newly synthesized compounds were characterized by ^{1}H NMR, ^{13}C NMR, ESI-MS, and HRMS.

2.2. Biological activity

2.2.1. Kinase inhibitory activity

The enzyme activity assays of new compounds were performed at a single-point concentration (1 μM) against EGFR and their inhibitory activities were displayed at Table 1. As shown in Table 1, compounds **12c**–**12e** and **13c**–**13d** exhibited favorable inhibition of the ErbB1 (percent inhibition values range of 99–102%), while compounds **7d**, **12a**, **12f**, **13a**, and **13b** showed moderate inhibitory activities (percentage of inhibition raning from 30% to 67%) and others had no obvious inhibitory activities.

Subsequently, we further evaluated the EGFR inhibitory activities of compounds **12c**–**12e** and **13c**–**13d** with excellent inhibition at 1 μM. As shown in Table 2, the IC_{50} values ranging from 2.97 to 108 nM against ErbB1 and EGFR (L858R). Compounds **12c**–**12e** and **13c**–**13d** were chosen for further evaluation of the selectivity of EGFR kinase, the IC_{50} values of **12c**–**12e** and **13c**–**13d** ranging from 590 to 1603 nM against HER2, and HER4, while compounds **12c**–**12e** and **13c**–**13d** had no obvious inhibitory activity toward EGFR (T790M/L858R). These results indicated that compounds **12c**–**12e** and **13c**–**13d** had good selectivity to EGFR kinase.

2.2.2. In vitro anti-proliferative activity

The antiproliferative activities of newly synthesized compounds were evaluated against a panel of five human cancer cell lines overexpressing EGFR, including MCF-7, A549, BT-474, SK-BR-3, and MDA-MB-231 by the standard MTT assay in vitro [17–19], with gefitinib as the positive control. The inhibitory activities (IC_{50}) were summarized in Table 1. As depicted in Table 1, the results indicated that most compounds showed moderate to good activity with IC_{50} values in the μM range, while compounds **7a**–**7d** proved to be ineffective against the five cell lines, and compounds **12c** and **18** also showed no inhibitory activity against A549 cell line (IC_{50} > 100 μM). Some of the synthesized compounds exhibited similar anti-proliferative activities as gefitinib against the three to four cell lines. Specifically compounds **6**, **12d**, **13a**–**13b**, **18**, and **19a**–**19b** showed higher antiproliferative activities than gefitinib against MCF-7 cell line. In addition, five compounds (**12c**–**12e** and **13c**–**13d**) exhibited remarkable inhibitory activity with the IC_{50}

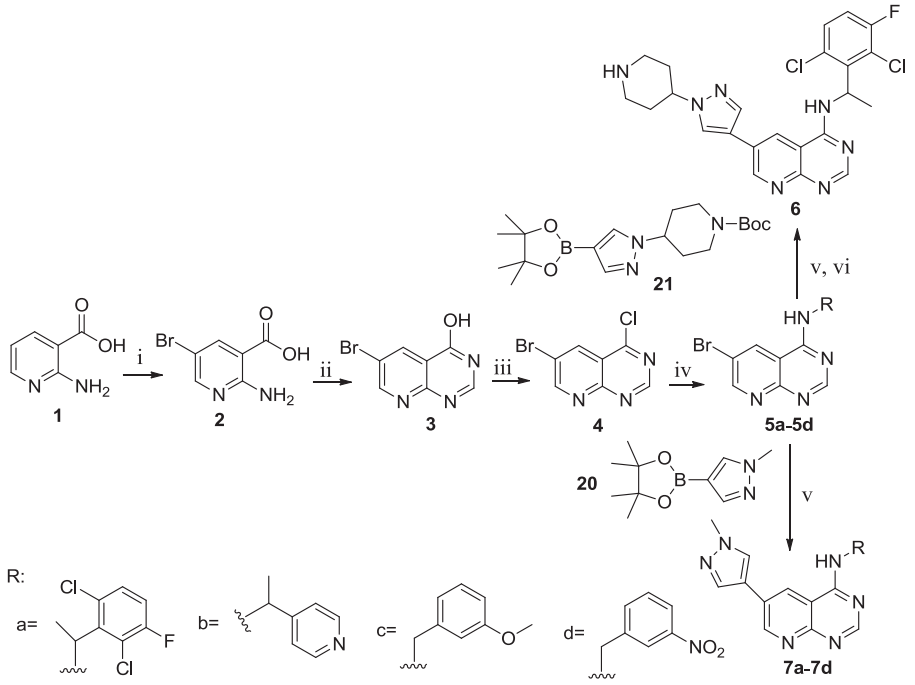

Scheme 1. Reagents and conditions: (i) bromine, acetic acid, rt; (ii) formamide, reflux; (iii) $SOCl_2$ and DMF, reflux; (iv) substituted-benzylamines, dioxane, rt; (v) K_2CO_3, $PdCl_2$(dppf) CH_2Cl_2, dioxane/H_2O (24:1), 85 °C; (vi) CH_2Cl_2/TFA (4:1), rt.

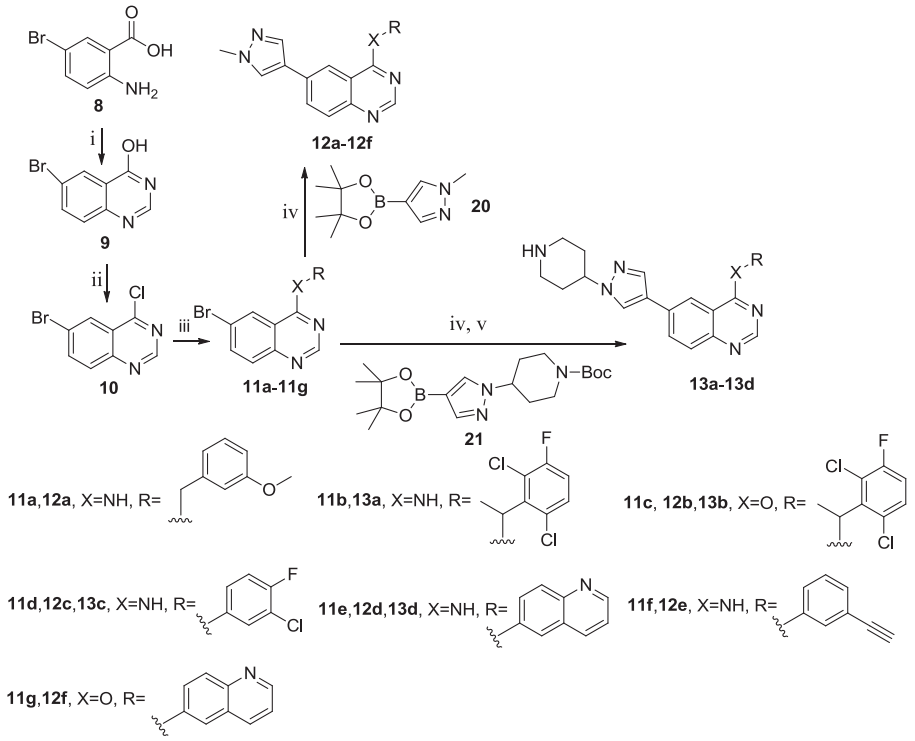

Scheme 2. Reagents and conditions: (i) formamide, reflux; (ii) $SOCl_2$ and DMF, reflux, (iii) for **11a**–**11b**, substituted-benzylamines, K_2CO_3, dioxane, rt; for **11c**, 1-(2,6-dichloro-3-fluorophenyl)- ethanol, dioxane, NaH, 0 °C-rt; for **11d**–**11f**, substituted-anilines or 6-aminoquinoline, acetone, HCl, reflux; for **11g**, Cs_2CO_3, dioxane, rt; (iv) K_2CO_3, $PdCl_2$(dppf) CH_2Cl_2, dioxane/H_2O (24:1), 85 °C; (v) CH_2Cl_2/TFA (4:1), rt.

values ranging from 0.064 to 5.87 μM, which were comparable to that of gefitinib (IC_{50} = 4.92 μM) on SK-BR-3 cell line. All the compounds displayed poor activities (IC_{50}: 3.00 − >100 μM) in BT-474 cancer cell line, as compared with gefitinib.

This primary screening revealed that 4-aminoquinazoline core derivatives exhibited strong EGFR enzymatic potency and anti-proliferative activities. Specifically aniline moieties and quinoline amino fragment at C-4 position of the quinazoline core showed

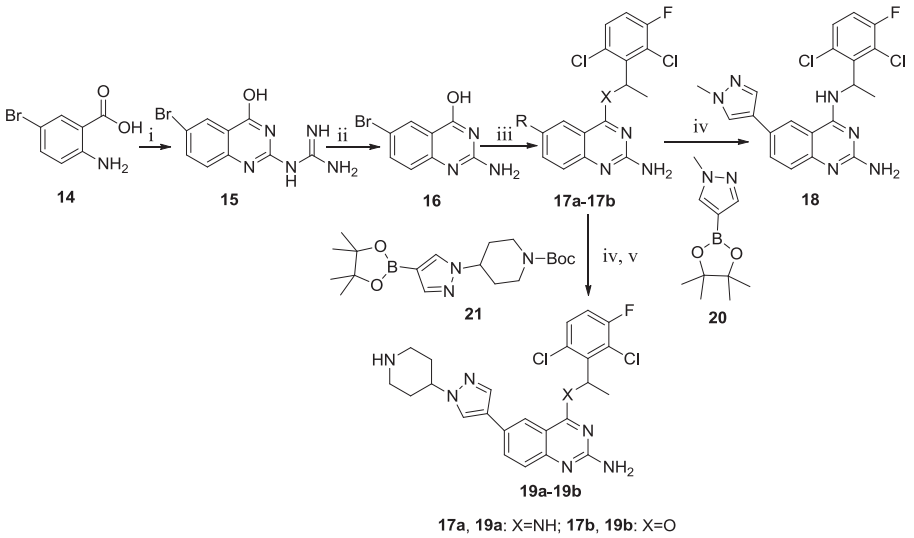

Scheme 3. Reagents and conditions: (i) dicyandiamide, sulfuric acid, 100 °C; (ii) 4-Pyridinethiol, KOH, ethylene glycol, 170 °C; (iii) for **17a**, BOP, DBU, 1-(2,6-Dichloro-3-fluorophenyl) ethan-1- amine, acetonitrile, rt; for **17b**, BOP, DBU, 1-(2,6-Dichloro-3-fluorophenyl)ethan-1-ol, NaH, acetonitrile, rt; (iv) K_2CO_3, $PdCl_2(dppf)CH_2Cl_2$, dioxane/H_2O (24:1), 85 °C; (v) CH_2Cl_2/TFA (4:1), rt.

promising inhibitory activity against EGFR and potent activity toward SK-BR-3 cell line, and had the makings of good drugs for breast cancer. The pyrido[2,3-*d*]pyrimidine derivatives displayed a significant loss in potency compared to that of 4-aminoquinazoline core derivatives. Moreover, 2-aminoquinazoline nucleus derivatives gave weak EGFR inhibitory activities. The enzymatic and cellular responses were inconsistent for some target compounds. Notably, compounds **6**, **13a**–**13b**, **18**, and **19a**–**19b** displayed poor activities against EGFR kinase, but they showed similar or higher antiproliferative activities than gefitinib against some cancer cell lines that express high levels of EGFR. It suggested that the compounds might induce cells apoptosis, or accelerate cell metabolism, or have some other mechanisms.

2.3. Preliminary structure–activity relationships

Based on biological activity evaluation of the synthetic compounds, the structure–activity relationships of these novel compounds were primarily analyzed. As shown in Fig. 2, the pyrido[2,3-*d*]pyrimidine derivatives show decreased inhibitory activity, and introduction of amino group at C-2 position of the quinazoline core did not led to significant inhibitory activity. Moreover, N-linker compounds showed good inhibitory activity than O-linker at C-4 position of scaffolds; aniline moieties directly conjunct to the 4-position of quinazoline core increased EGFR inhibitory activities as compared to benzyl amino groups. Interestingly, quinoline amino fragment at C-4 position of the quinazoline core also exhibited strong EGFR enzymatic and cellular potency.

2.4. Molecular modeling

To predict the possible binding mode of designed compounds with EGFR, a study of docking of all compounds into the active site of the EGFR (PDB ID: 4WKQ) were performed using Surflex-Dock and then molecular dynamics (MD) simulations were performed by using AMBER software package.

The docking reliability was validated using the known X-ray structure of EGFR complexed with gefitinib. The co-crystallized gefitinib was re-docked into the binding site, and the docked conformation with the highest total score was selected as the most probable binding conformation. As shown in Fig. 3, the redocked gefitinib is almost in the same position with co-crystallized gefitinib at the active site of EGFR except the flexible long chain extending into the solvent accessible region, which have revealed that the high reliability of Surflex-dock in reproducing the experimentally observed binding mode for the EGFR inhibitors. Therefore, Surflex-Dock method was used in search of the binding conformations of the newly synthesised compounds. All compounds, except 2-amino-quinazoline derivatives **18** and **19a**–**19b**, were successfully docked into the active site of EGFR (Fig. 4). As is shown in Fig. 4, quinazoline and pyrido[2,3-d]pyrimidine compounds share similar binding pattern in the binding pocket with the co-crystal ligand gefitinib in the reference crystal structure, while the 2-amino-quinazoline derivatives is shifted out of the binding pocket to the solvent surface, which may be the reason of the low potency of 2-amino-quinazoline compounds.

MD simulations were carried out on active inhibitors **12c** and **12e** in complex with EGFR to explore in depth the binding poses. For comparison, the MD simulations of positive control gefitinib and less active compound **7a** complexed with EGFR were also carried out.

MD simulations were processed in explicit aqueous solution for 20 ns. The stability of the system under simulation was evaluated by the root-mean-square deviation (RMSD) of the backbone atoms relate to the starting structures (Fig. 5). As can be seen in the plot, all systems reached equilibrium after 8 ns simulation times. Fig. 6 shows the binding poses of the two active compounds **12c** and **12e** in the binding pocket of EGFR. As illustrated in Fig. 6, the binding modes of **12c** and **12e** from MD simulated results are nearly the same as the docked structures. The quinazoline moiety inserts into deep hydrophobic pocket, the aniline moiety is deeply in the back of the ATP-binding pocket. The pyrazole substituent occupies the solvent exposed region, indicating that the introduction of hydrophilic groups here probably is beneficial for potency.

The hydrogen bond plays an important role in inhibitor binding to kinase [21]. The hydrogen-bond interactions were examined and found that N1 of quinazoline ring of gefitinib, **12c** and **12e** establish strong hydrogen interaction with the backbone NH of Met-793 in the hinge region of EGFR during all the MD simulation time (Table 3), while the key hydrogen–bond interaction could not be

Table 1
The kinase inhibitory activities and in vitro antiproliferative effects of synthesized compounds.

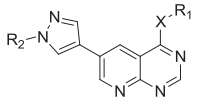

6, **7a-7d**

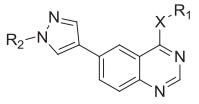

12a-12f, **13a-13d**

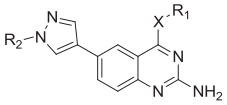

18, **19a-19b**

Com	X	R_1	R_2	EGFR inhibition at 1μM (%)[a]	In vitro antiproliferative effects (IC_{50}, μM)[b]				
					MCF-7	A549	BT-474	SK-BR-3	MDA-MB-231
6	NH			17	1.63	29.73	13.47	17.67	7.11
7a	NH		CH_3	9	>100	>100	>100	>100	>100
7b	NH		CH_3	0	>100	>100	>100	>100	>100
7c	NH		CH_3	18	>100	>100	>100	>100	>100
7d	NH		CH_3	30	>100	>100	>100	>100	>100
12a	NH		CH_3	67	40.04	48.90	30.40	35.95	28.49
12b	O		CH_3	11	22.55	28.79	45.60	27.20	30
12c	NH		CH_3	101	52.20	>100	5.26	3.10	62.65
12d	NH		CH_3	101	0.49	1.38	10.93	0.064	26.28
12e	NH		CH_3	102	11.37	9.86	5.68	5.87	16.93
12f	O		CH_3	43	21.97	26.63	24.30	14.42	16.51
13a	NH			61	2.65	7.00	8.13	4.39	12.60
13b	O			52	2.67	6.75	4.14	2.50	6.77
13c	NH			99	31.30	29.43	15.16	3.74	28.35
13d	NH			96	61.93	32.01	12.85	2.66	30.33
18	NH		CH_3	12	2.87	>100	7.12	7.14	7.96
19a	NH			17	2.23	8.80	5.10	1.58	4.48
19b	O			7	1.24	9.49	3.00	7.12	7.00
gefitinib				101	25.37	24.25	0.53	4.92	37.82

[a] Values are the average of two independent experiments.
[b] The data were means from at least three independent experiments.

Table 2
In vitro enzymatic inhibitory activities of compounds **12c**–**12e** and **13c**–**13d** against different types of EGFR.

Com	EGFR (IC_{50}, nM)[a]				
	EGFR (ErbB1)	EGFR (ErbB1) L858R	EGFR (ErbB1) L858R/T790M	ErbB2 (HER2)	ErbB4 (HER4)
12c	2.97	3.50	>1000	676	801
12d	44.1	108	>1000	874	930
12e	3.58	4.25	>1000	590	782
13c	31.9	39.1	>1000	1202	1603
13d	28.2	35.0	>1000	1350	1100
gefitinib	0.585	0.637	1013 [20]	1830 [20]	ND[b]

[a] Values are the average of two independent experiments.
[b] ND, not determined.

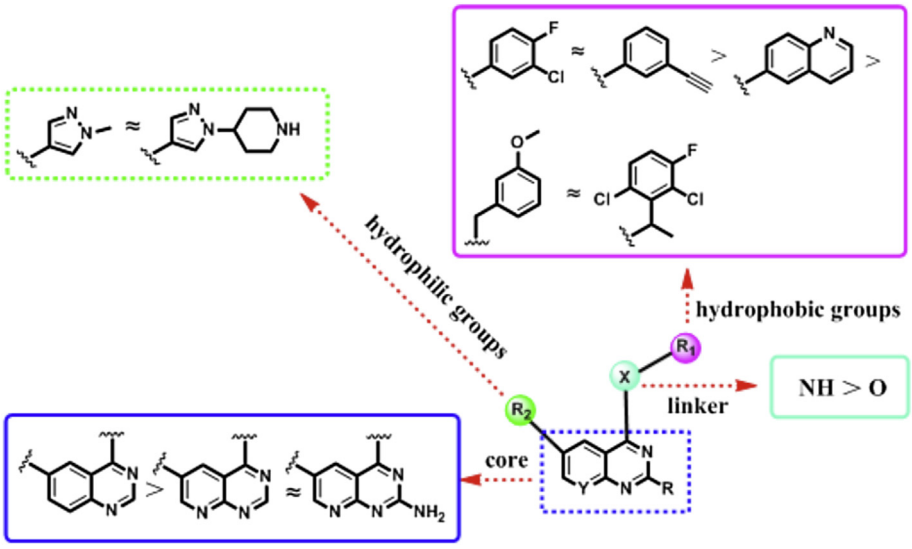

Fig. 2. Preliminary structure–activity relationships.

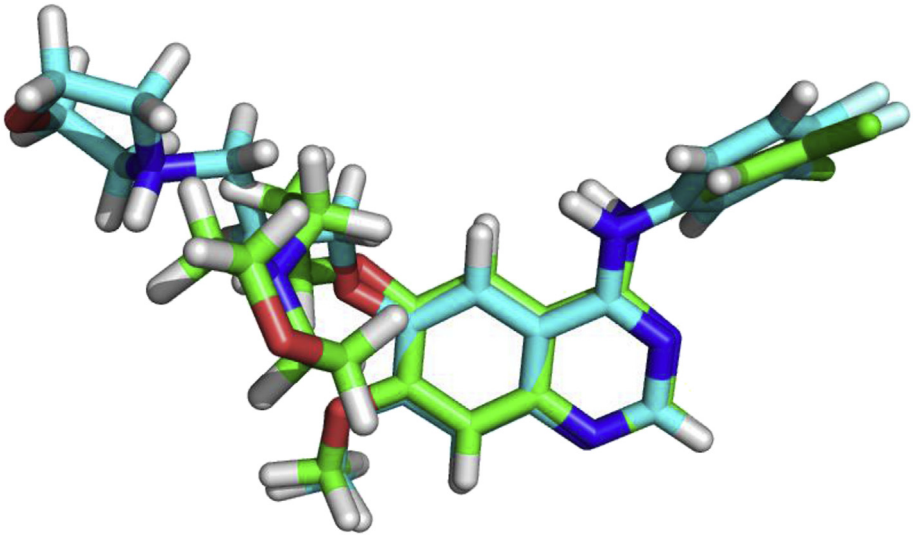

Fig. 3. Conformation comparison between redocked (cyan) and the co-crystallized (green) gefitinib binding to EGFR. (For interpretation of the references to color in this figure caption, the reader is referred to the web version of this article.)

formed in the system of **7a**-EGFR, which partically explains the low potency of compound **7a**.

The binding free energies were calculated by using MM-GBSA program in AMBER taking the last 10 ns of the MD simulation. In Table 4, we present the predicted binding free energies, together with their respective enthalpic and entropic contributions. As can been seen, MM-GBSA calculations verified that ligands **12c** and **12e** have almost the same activities against EGFR as the positive control

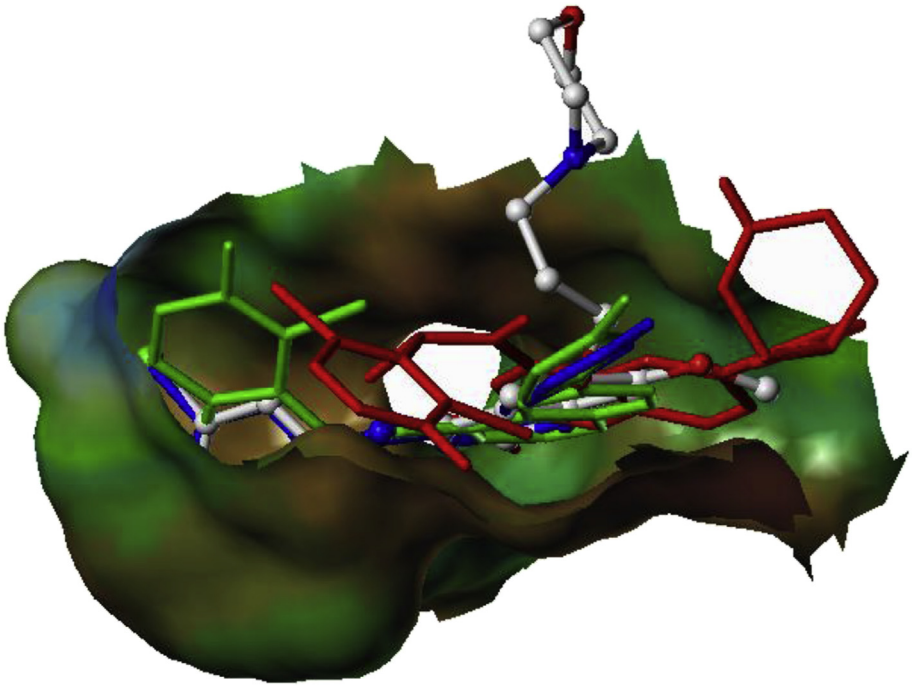

Fig. 4. Binding mode between EGFR kinase and representative compounds. (gefitinib in stick and ball model, **7a** in green stick model, **12c** in blue stick model, and **19a** in red stick model). (For interpretation of the references to color in this figure caption, the reader is referred to the web version of this article.)

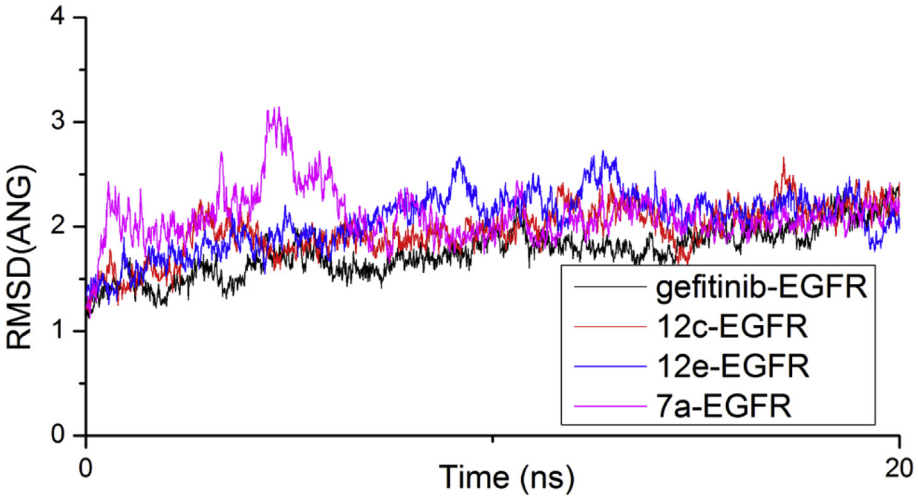

Fig. 5. RMSDs of backbone atoms (C, Cα, and N) of the systems against the initial structures.

gefitinib, which is in good agreement with the experimental data. In addition, the binding free energy of compound **7a** binding to EGFR is approximately 3 kcal/mol more than that of gefitinib, in consistent with the experimental observation that ligand **7a** exhibits drastically diminished potency.

According to the energy individual components of the binding free energies, the favorable contributors to ligand binding are van der Waals (vdW) terms, electrostatic and nonpolar salvation energies, whereas polar solvation and entropy terms oppose binding. The favorable electrostatic interactions are counteracted by the unfavorable electrostatics of desolvation upon binding. Consequently, the total electrostatic interaction contributions are unfavorable to binding in all systems. The vdW contribution interaction upon binding is very important to the binding of inhibitors with EGFR. Comparing **7a**-EGFR with the other complexes, the most important terms which dictates the difference in the binding affinity are ΔG_{ele} and ΔG_{vdW}.

3. Conclusion

In summary, three series of novel quinazoline and pyrido[2,3-*d*] pyrimidine derivatives were designed, synthesized and screened for biological activity as novel EGFR inhibitors. The preliminary investigation shows some compounds displayed favorable effect in the EGFR kinase assay and antiproliferative assay. Among them, compounds **12c** and **12e** showed the higher potency to EGFR kinase. In addition, the molecular docking and MD simulations experiments have revealed that the binding poses of **12c** and **12e** with EGFR are similar to that of gefitinib. MM-GBSA binding free energy revealed that the compound **12c** and **12e** have almost the same

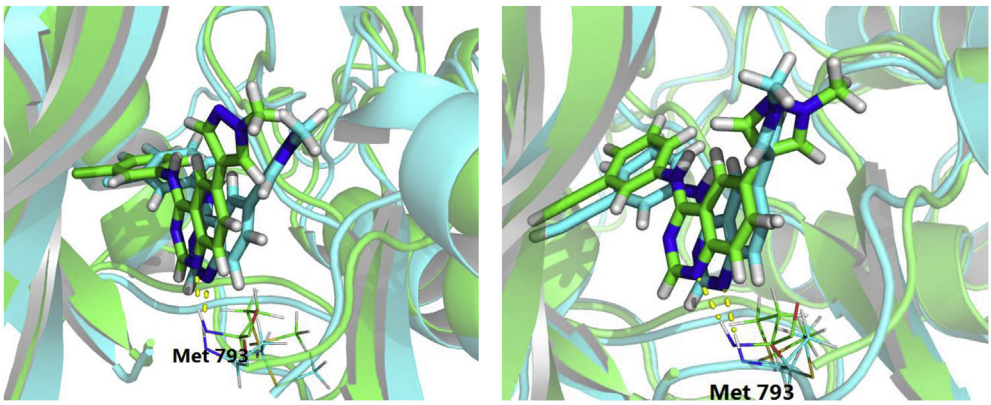

Fig. 6. Binding mode comparison between redocked (green) and MD simulated representative snapshots (cyan) of **12c** (left panel) and **12e** (right panel) in the active site of EGFR. Yellow dots represent hydrogen bonds. (EGFR in colored cartoon, ligands in stick model, the key residues in lines model). (For interpretation of the references to color in this figure caption, the reader is referred to the web version of this article.)

Table 3
Hydrogen Bonds analysis from MD.

	Donor	Acceptor	Distance (Å)[a]	Angle(°)[b]	Occupancy (%)[c]
gefitinib-EGFR	Met 793 NH	Ligand N	3.163(0.15)	24.38(11.31)	92.45
7a-EGFR	Met 793 NH	Ligand N	3.291(0.16)	34.78(15.22)	0.95
12c-EGFR	Met 793 NH	Ligand N	3.118(0.15)	22.17(12.34)	95.55
12e-EGFR	Met 793 NH	Ligand N	3.141(0.15)	26.30(13.19)	89.65

[a] The average distance with standard error (SE = standard deviation/$N^{1/2}$) in parentheses between hydrogen-acceptor atom and hydrogen-donor atom in the investigated time period.
[b] The average angle with standard error (SE = standard deviation/$N^{1/2}$) in parentheses for hydrogen bond in the investigated time period.
[c] Occupancy is in unit of percentage of the investigated time period.

Table 4
MM-GBSA binding free energies and its components for the studied complexes for the last 10 ns MD trajectories[a].

	ΔG_{vdW}	ΔG_{ele}	ΔG_{MM}	$\Delta G_{ele,sol}$	$\Delta G_{np,sol}$	ΔH_{pred}	$-T\Delta S$	ΔG_{pred}
gefitinib	−47.78 (0.10)	−90.05 (0.40)	−137.83 (0.43)	108.48 (0.41)	−6.17 (0.01)	−35.52 (0.10)	22.15 (2.94)	−13.37
7a	−41.51 (0.07)	−7.55 (0.08)	−49.06 (0.13)	25.89 (0.10)	−5.22 (0.01)	−28.39 (0.07)	18.33 (2.30)	−10.06
12c	−44.38 (0.08)	−11.42 (0.11)	−55.81 (0.14)	25.23 (0.11)	−5.51 (0.01)	−36.08 (0.08)	22.31 (0.61)	−13.77
12e	−45.29 (0.09)	−17.75 (0.08)	−63.04 (0.13)	33.16 (0.08)	−5.46 (0.01)	−35.34 (0.09)	22.22 (1.36)	−13.12

ΔH: the enthalpy changes, $\Delta H = \Delta G_{ele} + \Delta G_{vdW} + \Delta G_{np,sol} + \Delta G_{ele,sol}$.
TΔS: the entropy changes.
ΔG_{pred}: the calculated binding free energy by MM-GBSA method.
[a] Mean energies are in kcal/mol, with corresponding standard errors (SE = standard deviation/$N^{1/2}$) in parentheses.

inhibitory activity against EGFR as gefitinib, and that the dominating effect of vdW interactions drives the binding process. Compounds **12c** and **12e** could be worth of further development, and these results expand the chemical diversity of EGFR inhibitors.

4. Experimental

4.1. Chemistry

All reagents were purchased from commercial vendors and were used without further purification. All oxygen-sensitive or moisture-sensitive reactions were run under nitrogen atmosphere. ^1H and ^{13}C NMR spectra were recorded on a BRUKER AVIII 400 MHz and 101 MHz spectrometer with tetramethylsilane (TMS) as the internal standard, the values of the chemical shifts (δ) are given in ppm, and coupling constants (*J*) are given in Hz. Mass spectra (ESI-MS) were performed on WATERS ZQ4000. Highresolution mass spectra (HRMS) were recorded on AB Sciex TripleTOF 5600 mass spectrometer. All reactions were monitored using thin-layer chromatography (TLC) on silica gel plates at 254 nm under a UV laMp. Flach column chromatography separations were performed on normal phase silica gel (200–300 mesh, Merck) or reverse phase silica gel by using Yamazen AI-580 flash chromatography with UV detection at 254 nm. Melting points were determined using a X-4 Melting-point Apparatus with Microscope (Gongyi City Yuhua Instrument Co., Ltd., Hennan, China) and were uncorrected.

4.1.1. 1-(2,6-Dichloro-3-fluorophenyl)ethan-1-amine [15]

Preparation of 1-(2,6-Dichloro-3-fluorophenyl)ethan-1-amine and characteriza-tion data have already been reported. ^1H NMR (400 MHz, DMSO-d_6) δ 8.72 (s, 2H), 7.66 (dd, $J = 5.2, 9.2$ Hz, 1H), 7.58 (t, $J = 8.8$ Hz, 1H), 5.03 (q, $J = 6.8$ Hz, 1H), 1.63 (d, $J = 7.2$ Hz, 1H), ESI-MS *m/z*: 208.0 $[M+H]^+$.

4.1.2. 1-(pyridin-3-yl)ethanamine [22]

Preparation of 1-(pyridin-3-yl)ethanamine and characterization data have already been reported. ^1H NMR (400 MHz, MeOD) δ 8.48 (d, $J = 6.4$ Hz, 2H), 7.46 (d, $J = 6.0$ Hz, 2H), 4.08 (q, $J = 6.6$ Hz, 1H), 1.41 (d, $J = 6.8$ Hz, 3H), ESI-MS *m/z*: 123.2 $[M+H]^+$.

*4.1.3. 2-amino-5-bromonicotinic acid (**2**)*

Preparation of **2** and characterization data have already been reported. ^{1}H NMR (400 MHz, MeOD) δ 9.24 (d, J = 2.0 Hz, 1H), 9.14 (d, J = 2.0 Hz, 1H). ESI-MS m/z: 216.7 $[M+H]^+$.

*4.1.4. 6-bromopyrido[2,3-d]pyrimidin-4-ol (**3**)*

2-amino-5-bromonicotinic acid (**2**) (21.6 g, 0.10 mol) was added to a solution of formamide 100 mL, and then the reaction mixture was stirred at reflux for 5 h. The mixture was poured into 800 mL H_2O. The resulting precipitate was filtered, washed with water, and dried to give **3** as an off-white solid (16.9 g, yield, 74%). ^{1}H NMR (400 MHz, DMSO-d_6) δ 12.72 (s, 1H), 9.05 (d, J = 2.4 Hz, 1H), 8.63 (d, J = 2.4 Hz, 1H), 8.36 (s, 1H). ESI-MS m/z: 228.3 $[M+H]^+$.

*4.1.5. 6-bromo-4-chloropyrido[2,3-d]pyrimidine (**4**)*

To the suspension of 6-bromopyrido[2,3-d]pyrimidin-4-ol (**3**) (15.0 g, 0.066 mol) in thionyl chloride 150 mL was added a few drops of DMF, then the mixture was stirred at reflux for 6 h. After removing thionyl chloride under vacuum, the residue was recrystallized from EtOAc to gave **4** as pale yellow solid (11.8 g, yield, 73%). ^{1}H NMR (400 MHz, $CDCl_3$) δ 9.33 (d, J = 7.6 Hz, 2H), 8.80 (s, 1H). ESI-MS m/z: 246.9 $[M+H]^+$.

*4.1.6. 6-bromo-N-(1-(2,6-dichloro-3-fluorophenyl)ethyl)pyrido [2,3-d]pyrimidin-4-amine (**5a**)*

To a solution of compound **4** (2.43 g, 0.01 mol) in 25 mL dioxane was added 1-(2,6-Dichloro-3-fluorophenyl)ethan-1-amine (3.12 g, 0.015 mol), and then the reaction mixture was stirred at room temperature overnight. After that, the mixture was poured into 150 mL H_2O, and then the resulting precipitate was filtered, washed with 50% ethanol, and dried overnight under vacuum to give **5a** as white solid (3.58 g, yield, 86%). ^{1}H NMR (400 MHz, DMSO-d_6) δ 9.40 (d, J = 2.4 Hz, 1H), 9.07 (d, J = 2.0 Hz, 1H), 9.03 (d, J = 5.2 Hz, 1H), 8.48 (s, 1H), 7.47–7.44 (m, 1H), 7.35 (t, J = 8.8 Hz, 1H), 5.85 (q, J = 7.0 Hz, 1H), 1.71 (d, J = 7.2 Hz, 3H). ESI-MS m/z: 417.4 $[M+H]^+$.

*4.1.7. 6-bromo-N-(1-(pyridin-4-yl)ethyl)pyrido[2,3-d]pyrimidin-4-amine (**5b**)*

Compound **5b** was synthesized from **4** and 1-(pyridin-3-yl) ethanamine following the similar procedure described above for the preparation of **5a** (yield, 76%). ^{1}H NMR (400 MHz, DMSO-d_6) δ 9.27 (d, J = 2.4 Hz, 1H), 9.08 (d, J = 2.4 Hz, 1H), 8.90 (d, J = 7.4 Hz, 1H), 8.57 (s, 1H), 8.50 (dd, J = 1.6, 4.8 Hz, 2H), 7.43 (dd, J = 1.2, 4.4 Hz, 2H), 5.50 (q, J = 7.0 Hz, 1H), 1.60 (d, J = 7.2 Hz, 3H). ESI-MS m/z: 332.5 $[M+H]^+$.

*4.1.8. 6-bromo-N-(3-methoxybenzyl)pyrido[2,3-d]pyrimidin-4-amine (**5c**)*

Compound **5c** was synthesized from **4** and (3-methoxyphenyl) methanamine following the similar procedure described above for the preparation of **5a** (yield, 58%). ^{1}H NMR (400 MHz, DMSO-d_6) δ 9.16 (t, J = 5.6 Hz, 1H), 9.11 (d, J = 2.4 Hz, 1H), 9.07 (d, J = 2.4 Hz, 1H), 8.64 (s, 1H), 7.25 (t, J = 8.2 Hz, 1H), 6.96–6.95 (m, 2H), 6.86–6.85 (m, 1H), 4.77 (d, J = 5.6 Hz, 2H), 3.74 (s, 3H). ESI-MS m/z: 347.1 $[M+H]^+$.

*4.1.9. 6-bromo-N-(3-nitrobenzyl)pyrido[2,3-d]pyrimidin-4-amine (**5d**)*

Compound **5d** was synthesized from **4** and (3-nitrophenyl) methanamine following the similar procedure described above for the preparation of **5a** (yield, 72%). ^{1}H NMR (400 MHz, DMSO-d_6) δ 9.66 (s, 1H), 9.14 (d, J = 8.0 Hz, 2H), 8.72 (s, 1H), 8.28 (s, 1H), 8.15 (d, J = 7.6 Hz, 1H), 7.88 (d, J = 7.6 Hz, 1H), 7.65 (t, J = 7.8 Hz, 1H), 4.95 (d, J = 5.2 Hz, 2H). ESI-MS m/z: 362.3 $[M+H]^+$.

*4.1.10. N-(1-(2,6-dichloro-3-fluorophenyl)ethyl)-6-(1-(piperidin-4-yl)-1H-pyrazol-4-yl)pyrido[2,3-d]pyrimidin-4-amine (**6**)*

A mixture of compound **5a** (457 mg, 1.1 mmol), tert-Butyl 4-[4-(4,4,5,5-tetram- ethyl-1,3,2-dioxaborolan-2-yl)-1H-pyrazol-1-yl] piperidine-1-carboxylate (**21**) (400 mg, 1.06 mmol), $PdCl_2$(dppf) CH_2Cl_2 (80.2 mg, 0.098 mmol), and K_2CO_3 (420 mg, 3.04 mmol) in dioxane: H_2O (24:1) (12 mL) was degassed and charged with nitrogen for three times and then heated in an oil bath at 80 °C for 4 h under the protection of nitrogen. The reaction mixture was diluted with water (30 mL) and eracted with EtOAc (30 mL × 3). The combined organic layer was dried over anhydrous Na_2SO_4, filtered, and concentrated. The concentrates was purified by flash chromatography on silica gel eluting with petroleum ether-EtOAc-methnaol (containing 1% ammonia) (40:60:0.05) to give a compound as a white solid. The solid was dissolved in a mixed solvent system (CH_2Cl_2/TFA = 4:1, 20 mL), then the reaction mixture was stirred at room temperature overnight, and concentrated. The residue was triturated with acetone-petroleum ether (1:1) to give **6** as a white solid (231 mg, yield, 48%). mp 265–267 °C. ^{1}H NMR (400 MHz, DMSO-d_6) δ 11.22 (s, 1H), 10.13 (s, 1H), 9.42 (s, 1H), 9.21 (s, 1H), 8.78 (s, 2H), 8.39 (s, 1H), 7.49 (s, 1H), 7.39 (t, J = 7.2 Hz, 1H) 5.96 (s, 1H), 4.60 (s, 1H), 3.61 (s, 2H), 3.12 (s, 2H), 2.27 (s, 4H), 1.87 (d, J = 6.0 Hz, 3H). ^{13}C NMR (101 MHz, MeOD) δ 161.0, 158.5, 156.0, 155.1, 151.8, 146.4, 138.1, 137.1, 130.4, 129.9, 128.1, 127.6, 117.6, 116.0, 115.8, 109.2, 56.1, 51.3, 43.0, 28.9, 16.1. ESI-MS m/z: 486.5 $[M+H]^+$. HRMS, ESI$^+$, m/z: Calcd for $C_{23}H_{22}Cl_2FN_7$ $(M+H)^+$, 486.1371; found, 486.1368.

*4.1.11. N-(1-(2,6-dichloro-3-fluorophenyl)ethyl)-6-(1-methyl-1H-pyrazol-4-yl)pyrido[2,3-d]pyrimidin-4-amine (**7a**)*

A mixture of compound **5a** (208 mg, 0.50 mmol), 1-methyl-4-(4,4,5,5-tetrameth- yl-1,3,2-dioxaborolan-2-yl)-1H-pyrazole (**20**) (108 mg, 0.52 mmol), $PdCl_2$(dppf)- CH_2Cl_2 (40.1 mg, 0.05 mmol) and K_2CO_3 (207 mg, 1.5 mmol) in dioxane: H_2O (24:1) (15 mL) was degassed and charged with nitrogen for three times and then heated in an oil bath at 80 °C for 4 h under the protection of nitrogen. The reaction mixture was diluted with water (30 mL) and eracted with EtOAc (30 mL × 3). The combined organic layer was dried over anhydrous Na_2SO_4, filtered, and concentrated. The concentrates was purified by flash chromatography on silica gel eluting with petroleum ether-EtOAc-methnaol (containing 1% ammonia) (40:60:0.05) to give **7a** (129 mg, yield, 62%). mp 268–271 °C. ^{1}H NMR (400 MHz, MeOD) δ 9.20 (d, J = 2.0 Hz, 1H), 9.06 (d, J = 2.4 Hz, 1H), 8.43 (s, 1H), 8.21 (s, 1H), 8.07 (s, 1H), 7.35 (dd, J = 5.2, 8.8 Hz, 1H), 7.14 (t, J = 8.6 Hz, 1H), 6.07 (q, J = 7.4 Hz, 1H), 4.01 (s, 3H), 1.83 (d, J = 7.2 Hz, 3H). ^{13}C NMR (101 MHz, MeOD) δ 159.6, 157.2, 155.9, 152.9, 139.6, 136.5, 129.5, 129.4, 128.4, 127.1, 126.9, 118.8, 115.2, 114.9, 109.6, 49.3, 37.8, 16.3. ESI-MS m/z: 417.5 $[M+H]^+$. HRMS, ESI$^+$, m/z: Calcd for $C_{19}H_{15}Cl_2FN_6$ $(M+H)^+$, 417.0792; found, 417.0794.

*4.1.12. 6-(1-methyl-1H-pyrazol-4-yl)-N-(1-(pyridin-4-yl)ethyl) pyrido[2,3-d]pyrimidin-4-ami-ne (**7b**)*

Compound **7b** was synthesized from **5b** and **20** following the similar procedure described above for the preparation of **7a** (yield, 55%). mp 152–154 °C. ^{1}H NMR (400 MHz, MeOD) δ 9.20 (d, J = 9.6 Hz, 1H), 8.99 (s, 1H), 8.49 (d, J = 4.8 Hz, 3H), 8.20 (d, J = 7.6 Hz, 1H), 8.05 (d, J = 7.2 Hz, 1H), 7.52 (d, J = 5.6 Hz, 2H), 5.61 (q, J = 5.6 Hz, 1H), 4.00 (s, 3H), 1.74 (d, J = 7.2 Hz, 3H). ^{13}C NMR (101 MHz, MeOD) δ 160.3, 157.1, 156.0, 154.4, 153.1, 148.8, 136.5, 128.4, 127.1, 126.9, 121.7, 118.7, 109.8, 49.9, 37.8, 20.3. ESI-MS m/z: 332.6 $[M+H]^+$. HRMS, ESI$^+$, m/z: Calcd for $C_{18}H_{17}N_7$ $(M+H)^+$, 332.1618; found, 332.1621.

*4.1.13. N-(3-methoxybenzyl)-6-(1-methyl-1H-pyrazol-4-yl)pyrido [2,3-d]pyrimidin-4-amine (**7c**)*

Compound **7c** was synthesized from **5c** and **20** following the similar procedure described above for the preparation of **7a** (yield, 67%). mp 196–198 °C. ^{1}H NMR (400 MHz, DMSO-d_6) δ 9.28 (s, 1H), 9.11 (s, 1H), 8.99 (s, 1H), 8.58 (s, 1H), 8.32 (s, 1H), 8.03 (s, 1H), 7.26 (t, J = 8.0 Hz, 1H), 6.98 (s, 2H), 6.85 (d, J = 7.6 Hz, 1H), 4.82 (d, J = 5.6 Hz, 2H), 3.92 (s, 3H), 3.74 (s, 3H). ^{13}C NMR (101 MHz, DMSO-d_6) δ 161.1, 159.8, 157.6, 153.6, 140.9, 136.8, 129.9, 128.8, 126.9, 126.8, 120.0, 118.7, 113.9, 112.9, 110.0, 55.4, 44.4. ESI-MS m/z: 347.4 $[M+H]^+$. HRMS, ESI$^+$, m/z: Calcd for $C_{19}H_{18}N_6O$ $(M+H)^+$, 347.1615; found, 347.1619.

*4.1.14. 6-(1-methyl-1H-pyrazol-4-yl)-N-(3-nitrobenzyl)pyrido[2,3-d]pyrimidin-4-amine (**7d**)*

Compound **7d** was synthesized from **5d** and **20** following the similar procedure described above for the preparation of **7a** (yield, 74%). mp 290–293 °C. ^{1}H NMR (400 MHz, DMSO-d_6) δ 9.41 (s, 1H), 9.28 (d, J = 1.6 Hz, 1H), 9.05 (s, 1H), 8.54 (s, 1H), 8.35 (s, 1H), 8.27 (s, 1H), 8.13 (d, J = 8.0 Hz, 1H), 8.06 (s, 1H), 7.88 (d, J = 7.2 Hz, 1H), 7.64 (t, J = 7.8 Hz, 1H), 4.94 (s, 2H), 3.93 (s, 3H). ^{13}C NMR (101 MHz, DMSO-d_6) δ 161.0, 157.8, 157.0, 153.6, 148.3, 142.1, 136.8, 134.6, 130.3, 128.8, 127.0, 126.7, 122.4, 122.3, 118.7, 110.2, 66.8, 43.8. ESI-MS m/z: 362.2 $[M+H]^+$. HRMS, ESI$^+$, m/z: Calcd for $C_{18}H_{15}N_7O_2$ $(M+H)^+$, 362.1360; found, 362.1363.

*4.1.15. 6-bromoquinazolin-4-ol (**9**)*

Compound **9** was synthesized from **8** and formamide following the similar procedure described above for the preparation of **3**, and the crude product was directly used in the next step.

*4.1.16. 6-bromo-4-chloroquinazoline (**10**)*

Compound **10** was synthesized from **9** and thionyl chloride and DMF following the similar procedure described above for the preparation of **4** (yield, 75%). ^{1}H NMR (400 MHz, DMSO-d_6) δ 8.36 (s, 1H), 8.22 (d, J = 2.4 Hz, 1H), 8.01 (dd, J = 2.4, 8.8 Hz, 1H), 7.68 (d, J = 8.4 Hz, 1H), ESI-MS m/z: 244.9 $[M+H]^+$.

*4.1.17. 6-bromo-N-(3-methoxybenzyl)quinazolin-4-amine (**11a**)*

To a solution of compound **10** (2.43 g, 0.01 mol) in 25 mL dioxane was added (3-methoxyphenyl)methanamine (2.06 g, 0.015 mol) and K_2CO_3 (2.76 g, 0.02 mol), the reaction mixture was stirred at room temperature overnight. After that, the mixture was poured into 150 mL, and then the resulting precipitate was filtered, washed with 50% ethanol, and dried overnight under vacuum to give **11a** as white solid (2.33 g, yield, 68%). ^{1}H NMR (400 MHz, DMSO-d_6) δ 8.90 (t, J = 5.4 Hz, 1H), 8.63 (s, 1H), 8.50 (s, 1H), 7.90 (d, J = 8.8 Hz, 1H), 7.65 (d, J = 9.2 Hz, 1H), 7.24 (t, J = 8.0 Hz, 1H), 6.94 (d, J = 6.4 Hz, 2H), 6.82 (d, J = 7.6 Hz, 1H), 4.75 (d, J = 5.6 Hz, 2H), 3.73 (s, 3H). ESI-MS m/z: 344.4 $[M+H]^+$.

*4.1.18. 6-bromo-N-(1-(2,6-dichloro-3-fluorophenyl)ethyl) quinazolin-4-amine (**11b**)*

Compound **11b** was synthesized from **10** and 1-(2,6-Dichloro-3-fluorophenyl)et-han-1-amine following the similar procedure described above for the preparation of **11a** (yield, 71%). ^{1}H NMR (400 MHz, DMSO-d_6) δ 8.91 (d, J = 2.0 Hz, 1H), 8.76 (d, J = 5.6 Hz, 1H), 8.33 (s, 1H), 7.90 (dd, J = 2.0, 8.8 Hz, 1H), 7.61 (d, J = 9.2 Hz, 1H), 7.45–7.42 (m, 1H), 7.32 (t, J = 8.8 Hz, 1H), 5.85 (q, J = 7.2 Hz, 1H), 1.70 (d, J = 7.2 Hz, 3H). ESI-MS m/z: 416.4 $[M+H]^+$.

*4.1.19. 6-bromo-4-(1-(2,6-dichloro-3-fluorophenyl)ethoxy) quinazoline (**11c**)*

To a solution of 1-(2,6-Dichloro-3-fluorophenyl)ethan-1-ol (2.71 g, 0.013 mol) in 15 mL dioxane. The resulting solution was cooled at 0 °C and slowly added NaH (2.00 g, 0.03 mol, 60% dispersion in mineral oil) over 15 min. After complete addition, compound **10** was added. The mixture was stirred at 0 °C for 1 h and then stirred at room temperature overnight. The reaction mixture was poured into 100 mL H_2O, and the pH was adjusted to neutral with 10% aqueous hydrochloric acid. The resulting precipitate was filtered and washed with 50% ethanol, and dried overnight under high vacuum to give **11c** as white solid (3.30 g, yield, 79%). ^{1}H NMR (400 MHz, DMSO-d_6) δ 8.73 (s, 1H), 8.36 (d, J = 2.0 Hz, 1H), 8.10 (dd, J = 2.0, 8.8 Hz, 1H), 7.86 (d, J = 9.2 Hz, 1H), 7.54 (dd, J = 5.0, 9.2 Hz, 1H), 7.43 (t, J = 8.8 Hz, 1H), 6.90 (q, J = 6.8 Hz, 1H), 1.86 (d, J = 6.8 Hz, 3H). ESI-MS m/z: 417.6 $[M+H]^+$.

*4.1.20. 6-bromo-N-(3-chloro-4-fluorophenyl)quinazolin-4-amine (**11d**)*

To a solution of compound **10** (2.43 g, 0.01 mol) and 3-chloro-4-fluoroaniline 1.45 g (0.01 mol) in acetone: H_2O (4:1) (25 mL), followed by a few drops of hydrochloric acid. The reaction mixture stirred at reflux for 3 h, after cooling to room temperature, the pH was adjusted to neutral using ammonium hydroxide. The resulting precipitate was filtered and washed with water and dried overnight under high vacuum to give **11d** as a earthy yellow solid (2.80 g, yield, 80%). ^{1}H NMR (400 MHz, DMSO-d_6) δ 11.73 (s, 1H), 9.28 (d, J = 2.0 Hz, 1H), 8.97 (s, 1H), 8.23 (dd, J = 2.0, 8.8 Hz, 1H), 8.10 (dd, J = 2.4, 6.8 Hz, 1H), 7.94 (d, J = 9.2 Hz, 1H), 7.80 (ddd, J = 2.8, 4.4, 7.2 Hz, 1H), 7.55 (t, J = 9.0 Hz, 1H). ESI-MS m/z: 354.3 $[M+H]^+$.

*4.1.21. 6-bromo-N-(quinolin-6-yl)quinazolin-4-amine (**11e**)*

Compound **11e** was synthesized from **10** and 6-quinolylamine following the similar procedure described above for preparation of **11d** (yield, 74%). ^{1}H NMR (400 MHz, DMSO-d_6) δ 12.19 (s, 1H), 9.45 (d, J = 1.6 Hz, 1H), 9.19 (dd, J = 1.2, 4.8 Hz, 1H), 9.03 (s, 1H), 8.99 (d, J = 8.0 Hz, 1H), 8.71 (d, J = 2.0 Hz, 1H), 8.47 (dd, J = 2.0, 9.2 Hz, 1H), 8.41 (d, J = 9.2 Hz, 1H), 8.27 (dd, J = 2.0, 8.8 Hz, 1H), 8.01 (d, J = 8.8 Hz, 1H), 7.96 (dd, J = 5.2, 8.4 Hz, 1H). ESI-MS m/z: 353.7 $[M+H]^+$.

*4.1.22. 6-bromo-N-(3-ethynylphenyl)quinazolin-4-amine (**11f**)*

Compound **11f** was synthesized from **10** and 3-ethynylaniline following the same procedure described above for preparation of **11d** (yield, 86%). ^{1}H NMR (400 MHz, DMSO-d_6) δ 11.83 (s, 1H), 9.34 (d, J = 1.6 Hz, 1H), 8.99 (s, 1H), 8.25 (dd, J = 2.0, 8.8 Hz, 1H), 7.97 (d, J = 8.8 Hz, 1H), 7.94 (t, J = 1.6 Hz, 1H), 7.84–7.81 (m, 1H), 7.51 (t, J = 8.0 Hz, 1H), 7.44–7.42 (m, 1H), 4.30 (s, 1H). ESI-MS m/z: 326.2 $[M+H]^+$.

*4.1.23. 6-bromo-4-(quinolin-6-yloxy)quinazoline (**11g**)*

To a solution of 6-hydroxyquinoline (1.60 g, 0.011 mol) in 20 mL dioxane was added cesium carbonate (7.20 g, 0.022 mol). After stirring at room temperature for 1 h, compound **10** was added. The mixture was stirred at room temperature for a further overnight. The reaction mixture was poured into 200 mL H_2O, and pH was adjusted to neutral using aqueous hydrochloric acid. The resulting precipitate was filtered and washed with water and dried overnight under high vacuum to give **11g** as white solid (2.10 g, yield, 60%). ^{1}H NMR (400 MHz, DMSO-d_6) δ 8.96 (d, J = 2.8 Hz, 1H), 8.79 (s, 1H), 8.62 (d, J = 2.0 Hz, 1H), 8.41 (d, J = 8.0 Hz, 1H), 8.22 (dd, J = 2.0, 8.8 Hz, 1H), 8.16 (d, J = 9.2 Hz, 1H), 8.00 (d, J = 9.2 Hz, 2H), 7.82 (dd, J = 2.8, 9.2 Hz, 1H), 7.61 (dd, J = 4.0, 8.4 Hz, 1H). ESI-MS m/z: 354.8 $[M+H]^+$.

*4.1.24. N-(3-methoxybenzyl)-6-(1-methyl-1H-pyrazol-4-yl) quinazolin-4-amine (**12a**)*

Compound **12a** was synthesized from **11a** and **20** following the similar procedure described above for the preparation of **7a** (yield,

47%). mp 167–169 °C. ^{1}H NMR (400 MHz, DMSO-d_6) δ 8.71 (s, 1H), 8.53 (s, 1H), 8.41 (s, 1H), 8.20 (s, 1H), 7.99 (d, J = 8.8 Hz, 2H), 7.68 (d, J = 8.8 Hz, 1H), 7.25 (t, J = 7.6 Hz, 1H), 6.97 (s, 2H), 6.83 (d, J = 8.4 Hz, 1H), 4.81 (d, J = 3.6 Hz, 2H), 3.91 (s, 3H), 3.73 (s, 3H). ^{13}C NMR (101 MHz, DMSO-d_6) δ 159.8, 159.6, 154.8, 148.0, 141.5, 136.7, 130.6, 130.5, 129.9, 128.5, 128.4, 121.9, 119.8, 117.9, 115.6, 113.6, 112.5, 55.4, 43.9, 39.2. ESI-MS m/z: 346.2 $[M+H]^+$. HRMS, ESI$^+$, m/z: Calcd for $C_{20}H_{19}N_5O$ $(M+H)^+$, 346.1662; found, 346.1666.

4.1.25. 4-(1-(2,6-dichloro-3-fluorophenyl)ethoxy)-6-(1-methyl-1H-pyrazol-4-yl)quinazoline (**12b**)

Compound **12b** was synthesized from **11c** and **20** following the similar procedure described above for the preparation of **7a** (yield, 47%). mp 163–165 °C. ^{1}H NMR (400 MHz, DMSO-d_6) δ 8.62 (s, 1H), 8.36 (s, 1H), 8.30 (d, J = 2.0 Hz, 1H), 8.18 (dd, J = 2.0, 8.8 Hz, 1H), 8.02 (s, 1H), 7.88 (d, J = 8.8 Hz, 1H), 7.53 (dd, J = 4.8, 8.8 Hz, 1H), 7.42 (t, J = 8.8 Hz, 1H), 6.94 (q, J = 6.8 Hz, 1H), 3.93 (s, 3H), 1.88 (d, J = 7.2 Hz, 3H). ^{13}C NMR (101 MHz, DMSO-d_6) δ 164.9, 153.4, 149.6, 137.6, 136.9, 132.6, 129.1, 128.5, 121.2, 117.7, 117.5, 117.3, 116.6, 71.5, 39.2, 25.4, 18.5. ESI-MS m/z: 417.3 $[M+H]^+$. HRMS, ESI$^+$, m/z: Calcd for $C_{20}H_{15}Cl_2FN_4O$ $(M+H)^+$, 417.0680; found, 417.0685.

4.1.26. N-(3-chloro-4-fluorophenyl)-6-(1-methyl-1H-pyrazol-4-yl) quinazolin-4-amine (**12c**)

Compound **12c** was synthesized from **11d** and **20** following the similar procedure described above for the preparation of **7a** (yield, 69%). mp 209–211 °C. ^{1}H NMR (400 MHz, DMSO-d_6) δ 9.78 (s, 1H), 8.61 (d, J = 21.6 Hz, 2H), 8.22 (d, J = 23.6 Hz, 2H), 8.05 (s, 2H), 7.82 (d, J = 27.6 Hz, 2H), 7.46 (s, 1H), 3.93 (s, 3H). ^{13}C NMR (101 MHz, DMSO-d_6) δ 157.6, 155.0, 153.9, 152.6, 148.6, 136.9, 131.2, 128.8, 124.1, 122.9, 121.8, 119.4, 119.2, 117.7, 117.1, 116.9, 115.8, 39.9. ESI-MS m/z: 354.6 $[M+H]^+$. HRMS, ESI$^+$, m/z: Calcd for $C_{21}H_{16}N_6$ $(M+H)^+$, 354.0916; found, 354.0919.

4.1.27. 6-(1-methyl-1H-pyrazol-4-yl)-N-(quinolin-6-yl)quinazolin-4-amine (**12d**)

Compound **12d** was synthesized from **11e** and **20** following the similar procedure described above for the preparation of **7a** (yield, 79%). mp 263–265 °C. ^{1}H NMR (400 MHz, DMSO-d_6) δ 10.02 (s, 1H), 8.84 (dd, J = 1.6, 4.0 Hz, 1H), 8.78 (d, J = 1.6 Hz, 1H), 8.65 (s, 1H), 8.57 (d, J = 2.0 Hz, 1H), 8.37 (d, J = 7.6 Hz, 1H), 8.31 (s, 1H), 8.24 (dd, J = 2.0, 8.8 Hz, 1H), 8.17–8.07 (m, 3H), 7.82 (d, J = 8.8 Hz, 1H), 7.53 (dd, J = 4.0, 8.0 Hz, 1H), 3.95 (s, 3H). ^{13}C NMR (101 MHz, DMSO-d_6) δ 157.8, 154.1, 149.7, 148.7, 145.4, 137.7, 136.9, 135.9, 131.4, 131.2, 129.5, 128.8, 128.6, 126.6, 122.2, 121.8, 118.6, 117.9, 116.0, 99.9, 39.2. ESI-MS m/z: 353.6 $[M+H]^+$. HRMS, ESI$^+$, m/z: Calcd for $C_{21}H_{16}N_6$ $(M+H)^+$, 353.1509; found, 353.1512.

4.1.28. N-(3-ethynylphenyl)-6-(1-methyl-1H-pyrazol-4-yl) quinazolin-4-amine (**12e**)

Compound **12e** was synthesized from **11f** and **20** following the similar procedure described above for the preparation of **7a**. The crude product was purified by flash chromatography on C_{18} reverse phase silica gel eluting with 35% methnaol/water (50 mmol ammonium acetate adjusted to pH = 4 with formic acid) to give compound **12e** (yield, 37%). mp 118–121 °C. ^{1}H NMR (400 MHz, DMSO-d_6) δ 9.79 (s, 1H), 8.70 (s, 1H), 8.60 (s, 1H), 8.28 (s, 1H), 8.10–8.06 (m, 3H), 7.96 (d, J = 8.0 Hz, 1H), 7.79 (d, J = 8.4 Hz, 1H), 7.45 (t, J = 7.8 Hz, 1H), 7.27 (d, J = 7.6 Hz, 1H), 4.23 (s, 1H), 3.93 (s, 3H). ^{13}C NMR (101 MHz, DMSO-d_6) δ 157.7, 153.9, 148.3, 139.8, 136.9, 131.4, 131.3, 129.4, 128.8, 128.6, 127.3, 125.5, 123.3, 122.3, 121.8, 117.8, 115.9, 83.8, 81.1, 39.2. ESI-MS m/z: 326.6 $[M+H]^+$. HRMS, ESI$^+$, m/z: Calcd for $C_{21}H_{16}N_6$ $(M+H)^+$, 326.1400; found, 326.1406.

4.1.29. 6-(1-methyl-1H-pyrazol-4-yl)-4-(quinolin-6-yloxy) quinazoline (**12f**)

Compound **12f** was synthesized from **11g** and **20** following the same procedure described above for preparation of **7a** (yield, 83%). mp 209–211 °C. ^{1}H NMR (400 MHz, DMSO-d_6) δ 8.96 (dd, J = 1.6, 4.0 Hz, 1H), 8.67 (s, 1H), 8.55 (d, J = 2.0 Hz, 1H), 8.49 (s, 1H), 8.42 (dd, J = 1.2, 6.8 Hz, 1H), 8.31 (dd, J = 2.0, 8.8 Hz, 1H), 8.16 (t, J = 4.6 Hz, 2H), 8.02 (dd, J = 4.4, 7.2 Hz, 2H), 7.83 (dd, J = 2.4, 8.8 Hz, 1H), 7.61 (dd, J = 4.0, 8.4 Hz, 1H), 3.92 (s, 3H). ^{13}C NMR (101 MHz, DMSO-d_6) δ 166.6, 153.3, 150.9, 150.4, 150.2, 146.2, 137.1, 136.1, 133.1, 132.9, 131.0, 129.4, 128.9, 128.6, 126.1, 122.4, 121.1, 119.4, 117.6, 116.6, 39.2. MS: m/z (ESI+) 354.5 $[M+H]^+$. HRMS, ESI$^+$, m/z: Calcd for $C_{21}H_{15}N_5O$ $(M+H)^+$, 354.1349; found, 354.1348.

4.1.30. N-(1-(2,6-dichloro-3-fluorophenyl)ethyl)-6-(1-(piperidin-4-yl)-1H-pyrazol-4-yl)quinazolin-4-amine (**13a**)

Compound **13a** was synthesized from **11b** and **21** following the similar procedure described above for the preparation of **6** (yield, 79%). mp 185–188 °C. ^{1}H NMR (400 MHz, MeOD) δ 8.65 (d, J = 1.6 Hz, 1H), 8.29 (s, 2H), 8.15 (s, 1H), 8.03 (dd, J = 2.0, 8.4 Hz, 1H), 7.70 (d, J = 8.8 Hz, 1H), 7.35 (dd, J = 4.8, 8.8 Hz, 1H), 7.13 (t, J = 8.6 Hz, 1H), 6.10 (q, J = 7.2 Hz, 1H), 4.64 (ddd, J = 4.4, 12.6, 17.0 Hz, 1H), 3.61 (dt, J = 3.2, 16.4 Hz, 2H), 3.27 (td, J = 3.6, 12.8 Hz, 2H), 2.45–2.30 (m, 4H), 1.84 (d, J = 7.2 Hz, 3H). ^{13}C NMR (101 MHz, MeOD) δ 158.6, 158.4, 155.9, 154.0, 146.8, 140.0, 136.9, 130.8, 130.5, 129.4, 129.3, 126.7, 126.0, 122.1, 117.6, 115.0, 114.8, 55.7, 49.1, 42.8, 28.9, 16.4. ESI-MS m/z: 485.5 $[M+H]^+$. HRMS, ESI$^+$, m/z: Calcd for $C_{24}H_{23}Cl_2FN_6$ $(M+H)^+$, 485.1418; found, 485.1420.

4.1.31. 4-(1-(2,6-dichloro-3-fluorophenyl)ethoxy)-6-(1-(piperidin-4-yl)-1H-pyrazol-4-yl)quinazoline (**13b**)

Compound **13b** was synthesized from **11c** and **21** following the similar procedure described above for the preparation of **6** (yield, 50%). mp 157–158 °C. ^{1}H NMR (400 MHz, MeOD) δ 8.56 (s, 1H), 8.39 (s, 1H), 8.26 (s, 1H), 8.14 (dd, J = 1.2, 8.4 Hz 1H), 7.99 (s, 1H), 7.85 (d, J = 8.8 Hz, 1H), 7.41 (dd, J = 4.8, 8.8 Hz, 1H), 7.21 (t, J = 8.6 Hz, 1H), 7.02 (q, J = 6.8 Hz, 1H), 4.49–4.42 (m, 1H), 3.36 (d, J = 7.2 Hz, 1H), 3.29 (s, 1H), 2.96–2.90 (m, 2H), 2.25–2.01 (m, 5H), 1.94 (d, J = 6.8 Hz, 3H). ^{13}C NMR (101 MHz, MeOD) δ 165.3, 158.5, 156.0, 153.1, 148.9, 138.5, 137.5, 136.3, 132.1, 129.8, 128.7, 127.0, 125.7, 121.3, 118.0, 116.5, 104.9, 72.0, 58.4, 44.1, 31.7, 17.0. ESI-MS m/z: 486.6 $[M+H]^+$. HRMS, ESI$^+$, m/z: Calcd for $C_{24}H_{22}Cl_2FN_5O$ $(M+H)^+$, 486.1258; found, 486.1254.

4.1.32. N-(3-chloro-4-fluorophenyl)-6-(1-(piperidin-4-yl)-1H-pyrazol-4-yl)quinazolin-4-amin-e (**13c**)

Compound **13c** was synthesized from **11d** and **21** following the similar procedure described above for the preparation of **6** (yield, 63%). mp 293–296 °C. ^{1}H NMR (400 MHz, DMSO-d_6) δ 9.82 (s, 1H), 8.67 (d, J = 1.4 Hz, 1H), 8.59 (s, 1H), 8.36 (s, 1H), 8.20 (dd, J = 2.4, 6.8 Hz, 1H), 8.12 (dd, J = 2.0, 8.8 Hz, 1H), 8.08 (s, 1H), 7.87 (ddd, J = 2.4, 5.6, 7.6 Hz, 1H), 7.79 (d, J = 8.8 Hz, 1H), 7.47 (t, J = 9.2 Hz, 1H), 4.29–4.22 (m, 1H), 3.10–2.99 (m, 3H), 2.66–2.55 (m, 2H), 2.03 (d, J = 10.0 Hz, 2H), 1.89–1.82 (m, 2H). ^{13}C NMR (101 MHz, DMSO-d_6) δ 157.6, 155.0, 153.9, 152.6, 148.6, 136.5, 131.6, 128.7, 125.8, 124.1, 123.0, 121.2, 119.4, 117.7, 117.1, 116.9, 115.8, 59.8, 45.4, 33.9, 33.7, 22.9. ESI-MS m/z: 423.5 $[M+H]^+$. HRMS, ESI$^+$, m/z: Calcd for $C_{24}H_{22}Cl_2FN_5O$ $(M+H)^+$, 423.1495; found, 423.1499.

4.1.33. 6-(1-(piperidin-4-yl)-1H-pyrazol-4-yl)-N-(quinolin-6-yl) quinazolin-4-amine (**13d**)

Compound **13d** was synthesized from **11e** and **21** following the similar procedure described above for the preparation of **6** (yield, 63%). mp 126–127 °C. ^{1}H NMR (400 MHz, DMSO-d_6) δ 10.02 (s, 1H), 8.84 (dd, J = 1.6, 4.4 Hz, 1H), 8.78 (d, J = 1.2 Hz, 1H), 8.64 (s, 1H), 8.57

(d, J = 2.0 Hz, 1H), 8.39–8.35 (m, 2H), 8.25 (dd, J = 2.4, 9.2 Hz, 1H), 8.16–8.12 (m, 2H), 8.07 (d, J = 9.2 Hz, 1H), 7.81 (d, J = 8.4 Hz, 1H), 7.52 (dd, J = 4.0, 8.0 Hz, 1H), 4.29–4.24 (m, 1H), 3.09 (d, J = 12.0 Hz, 2H), 2.63 (t, J = 11.8 Hz, 2H), 2.06–2.03 (m, 2H), 1.90–1.81 (m, 2H). ^{13}C NMR (101 MHz, DMSO-d_6) δ 157.8, 154.0, 149.6, 148.7, 145.4, 137.7, 136.6, 135.9, 131.6, 131.3, 129.4, 128.8, 128.6, 126.6, 125.8, 122.2, 121.3, 118.6, 117.9, 116.0, 59.8, 45.4, 33.9. ESI-MS m/z: 422.7 $[M+H]^+$. HRMS, ESI$^+$, m/z: Calcd for $C_{25}H_{23}N_7$ $(M+H)^+$, 422.2088; found, 422.2093.

4.1.34. N-(6-bromo-4-hydroxyquinazolin-2-yl)guanidine (**15**)

To the mixture of 2-amino-5-bromobenzoic acid (**14**) (15.0 g, 0.07 mol), water 150 mL and concentrated sulfuric acid (8 mL) was heated at 100 °C before being allowed to cool. Dicyandiamide was added, and the reaction mixture was stirred for 2 h at 100 °C. The reaction was cooled and filtered. The white solid was basified with 100 mL (4 mol/L) NaOH at 180 °C for a further 15 min, cooled to room temperature, filtered and washed with water until neutral pH, and dried overnight under vacuum to give **15** as white solid 11.8 g, which was directly used in the next step.

4.1.35. 2-amino-6-bromoquinazolin-4-ol (**16**)

To a solution of N-(6-Bromo-4-hydroxyquinazolin-2-yl)guanidine (**15**) (8.00 g, 0.028 mol) and 4-Pyridinethiol (6.20 g, 0.056 mol) in ethylene glycol, KOH (7.80 g, 0.14 mol) was added. The resulting reaction mixture was stirred at 170 °C for about 4 h, cooled to room temperature, poured into 500 mL H_2O, and the pH was adjusted to neutral using hydrochloric acid. The resulting precipitate was filtered, washed with water and 50% ethanol, and dried overnight under high vacuum to give **16** as off-white solid (4.60 g, yield, 68%). ^{1}H NMR (400 MHz, DMSO-d_6) δ 11.11 (s, 1H), 7.97 (d, J = 2.4 Hz, 1H), 7.69 (dd, J = 2.8, 8.8 Hz, 1H), 7.57 (s, 2H), 7.30 (d, J = 8.8 Hz, 1H). ESI-MS m/z: 242.0 $[M+H]^+$.

4.1.36. 2-amino-6-bromo-N-(1-(2,6-dichloro-3-fluorophenyl)ethyl) quinazoline-4-amine (**17a**)

To a solution of compound **16** (1.20 g, 0.005 mol) and benzotriazol-1-yloxytris- (dimethylamino)-phosphonium hexafluorophosphat (BOP) (2.90 g, 0.0065 mol) in 20 mL acetonitrile, 1,8-Diazabicyclo-[5.4.0]undec-7-ene (DBU) (1.1 mL, 0.0075 mol) was added and the solution became clear. When precipitated solid was formed, 1-(2,6-Dichloro-3-fluoro-phenyl)-ethan-1-amine (1.56 g, 0.0075 mol) was added to the reaction mixture. The reaction mixture was stirred at room temperature overnight, then poured into 100 mL H_2O and extracted with EtOAc (30 mL × 3). The combined organic layer was dried over anhydrous Na_2SO_4, filtered, and concentrated. The crude product was purified by flash chromatography on silica gel eluting with Petroleum ether:DCM:EtOAc (2:1:2) to give **17a** (0.97 g, yield, 45%). ^{1}H NMR (400 MHz, DMSO-d_6) δ 8.60 (d, J = 2.4 Hz, 1H), 8.46 (d, J = 5.6 Hz, 1H), 8.17 (s, 1H), 7.62 (dd, J = 2.4, 9.2 Hz, 1H), 7.42 (dd, J = 4.8, 8.8 Hz, 1H), 7.32 (t, J = 8.8 Hz, 1H), 7.15 (d, J = 8.8 Hz, 1H), 5.94 (s, 1H), 5.82 (q, J = 6.4 Hz, 1H), 1.67 (d, J = 7.4 Hz, 3H). ESI-MS m/z: 431.4 $[M+H]^+$.

4.1.37. 6-bromo-4-(1-(2,6-dichloro-3-fluorophenyl)ethoxy) quinazolin-2-amine (**17b**)

To a solution of compound **16** (1.20 g, 0.005 mol) and benzotriazol-1-yloxytris(di-methylamino)-phosphonium hexafluorophosphat (BOP) (2.90 g, 0.0065 mol) in 20 mL acetonitrile, 1,8-Diazabicyclo[5.4.0]undec-7-ene (DBU) (1.1 mL, 0.0075 mol) was added and the solution became clear. When precipitated solid was formed, the solution of 1-(2,6-Dichloro-3-fluorophenyl)-ethan-1-ol (1.56 g, 0.0075 mol) and NaH (0.40 g, 60% dispersion in mineral oil) in 10 mL acetonitrile was added, and then stirred at room temperature overnight. The reaction mixture was poured into 100 mL H_2O and extracted with EtOAc (30 mL × 3). The combined organic layer was dried over anhydrous Na_2SO_4, filtered, and concentrated. The crude product was purified by flash chromatography on silica gel eluting with petroleum ether:DCM:EtOAc (2:1:2) to give **17b** (1.2 g, yield, 55%). ^{1}H NMR (400 MHz, $CDCl_3$) δ 8.23 (d, J = 2.0 Hz, 1H), 7.70 (dd, J = 2.4, 9.2 Hz, 1H), 7.35 (d, J = 8.8 Hz, 1H), 7.27 (dd, J = 5.2, 8.8 Hz, 1H), 7.05 (t, J = 8.4 Hz, 1H), 6.86 (q, J = 6.8 Hz, 1H), 4.99 (s, 2H), 1.91 (d, J = 6.9 Hz, 3H). ESI-MS m/z: 432.4 $[M+H]^+$.

4.1.38. 2-amino-N-(1-(2,6-dichloro-3-fluorophenyl)ethyl)-6-(1-methyl-1H-pyrazol-4-yl)quinazoline-4-amine (**18**)

Compound **18** was synthesized from **17a** and **20** following the similar procedure described above for the preparation of **7a** (yield, 51%). mp 269–272 °C. ^{1}H NMR (400 MHz, MeOD) δ 8.43 (d, J = 2.0 Hz, 1H), 8.01 (s, 1H), 7.96 (s, 1H), 7.81 (dd, J = 1.6, 8.4 Hz, 1H), 7.38–7.30 (m, 2H), 7.14 (t, J = 8.6 Hz, 1H), 6.04 (q, J = 7.3 Hz, 1H), 3.97 (s, 3H), 1.80 (d, J = 7.2 Hz, 3H). ^{13}C NMR (101 MHz, MeOD) δ 159.6, 158.6, 155.9, 146.8, 139.9, 136.0, 130.7, 129.3, 127.6, 127.0, 122.5, 122.4, 118.3, 115.1, 114.9, 110.7, 48.9, 37.6, 16.2. ESI-MS m/z: 431.5 $[M+H]^+$. HRMS, ESI$^+$, m/z: Calcd for $C_{20}H_{17}Cl_2FN_6$ $(M+H)^+$, 431.0949; found, 431.0950.

4.1.39. 2-amino-N-(1-(2,6-dichloro-3-fluorophenyl)ethyl)-6-(1-(piperidin-4-yl)-1H-pyrazol-4-yl)quinazoline-4-amine (**19a**)

Compound **19a** was synthesized from **17a** and **21** following the similar procedure described above for the preparation of **6** (yield, 74%). mp 113–115 °C. ^{1}H NMR (400 MHz, MeOD) δ 8.69 (s, 1H), 8.24 (s, 1H), 8.07–8.03 (m, 2H), 7.47–7.39 (m, 2H), 7.18 (dd, J = 8.4, 17.2 Hz, 1H), 6.09 (q, J = 7.2 Hz, 1H), 4.65–4.63 (m, 1H), 3.64–3.53 (m, 3H), 3.37 (s, 1H), 3.28–3.17 (m, 2H), 2.66 (d, J = 9.6 Hz, 1H), 2.40–2.25 (m, 5H), 1.84 (d, J = 7.2 Hz, 3H). ^{13}C NMR (101 MHz, MeOD) δ 138.8, 137.2, 136.6, 132.4, 129.9, 129.7, 127.9, 125.8, 121.2, 119.3, 117.2, 115.6, 115.4, 114.3, 110.0, 55.7, 49.8, 42.7, 42.6, 28.8, 28.6, 16.0. ESI-MS m/z: 500.5 $[M+H]^+$. HRMS, ESI$^+$, m/z: Calcd for $C_{24}H_{24}Cl_2FN_7$ $(M+H)^+$, 500.1527; found, 500.1528.

4.1.40. 4-(1-(2,6-dichloro-3-fluorophenyl)ethoxy)-6-(1-(piperidin-4-yl)-1H-pyrazol-4-yl)quinazolin-2-amine (**19b**)

Compound **19b** was synthesized from **17b** and **21** following the similar procedure described above for the preparation of **6** (yield, 65%). mp 267–269 °C. ^{1}H NMR (400 MHz, DMSO-d_6) δ 8.23 (s, 1H), 8.06 (d, J = 2.0 Hz, 1H), 7.89–7.87 (m, 2H), 7.55 (dd, J = 5.2, 8.8 Hz, 1H), 7.44 (t, J = 8.8 Hz, 1H), 7.34 (d, J = 8.8 Hz, 1H), 6.94 (q, J = 6.8 Hz, 1H), 6.39 (s, 2H), 4.34–4.28 (m, 1H), 3.16 (d, J = 14.4 Hz, 3H), 2.76–2.70 (m, 2H), 2.06–1.91 (m, 4H), 1.85 (d, J = 7.2 Hz, 3H). ^{13}C NMR (101 MHz, MeOD) δ166.2, 159.5, 158.6, 151.2, 137.5, 136.3, 132.0, 129.9, 128.9, 126.8, 125.3, 123.7, 122.2, 119.0, 116.2, 116.0, 111.5, 71.4, 56.1, 43.0, 29.4, 16.9. ESI-MS m/z: 501.4 $[M+H]^+$. HRMS, ESI$^+$, m/z: Calcd for $C_{24}H_{23}Cl_2FN_6O$ $(M+H)^+$, 501.1367; found, 501.1369.

4.2. Kinase inhibitory activity

The EGFR inhibitory activity was evaluated by using the Z'-LYTE technology platform (Life Technologies), and gefitinib was employed as the positive control. The experiments were performed according to the instructions of the manufacturer, and single point concentration testing (1 μM) with two independent data points (n = 2). According to the antiproliferative activities and percent inhibition values of compounds, we chosen compounds **12c**–**12e** and **13c**–**13d** to evaluate kinase activity at ten concentration gradients from 1000 to 0.0508 nM (3-fold dilution). The IC_{50} values were calculated from the inhibition curves from two separate experiments.

4.3. Cancer cell proliferation inhibition assay

The antiproliferative activities of compounds were evaluated against MCF-7, A549, BT-474, SK-BR-3 and MDA-MB-231 cell lines by the standard MTT assay in vitro, with gefitinib as the positive control. All cell lines were purchased from Cell Bank of China Science Academy (Shanghai, China). All chemicals and solvents were purchased from Sigma–Aldrich or Gibco.

The BT-474 cell line was maintained in DEME medium supplement with 10% fetal bovine serum (FBS) and 1% Penicillin-Streotomycin, others were cultured in RPMI 1640 medium also supplement with 10% FBS and 1% Penicillin-Streotomycin. Approximate 5×10^3 cells, suspended in medium, were plated into each well of a 96-well plate and grown at 37 °C in a humidified atmosphere with 5% CO_2 for 24 h. The following day various concentrations of tested compounds were added to the culture medium and incubated for 72 h. Fresh MTT was added to each well at the terminal concentration of 5 mg/mL in PBS, and incubated with cells at 37 °C for 4 h. The formazan crystals in each well were dissolved in 150 μL DMSO, and the absorbency at 570 nm was measured with an enzyme-linked immunosorbent assay plate reader. All of the compounds were tested three times in each of the cell lines.

4.4. Molecular modeling

Molecular docking was performed with Surflex-Dock program that is interfaced with Sybyl 7.3 [23] according to our previously published protocol [24]. The crystal structure of EGFR kinase in complex with gefitinib (ID: 4WKQ) was obtained from protein data bank (PDB) [25]. All the water and ligands were removed and the random hydrogen atoms were added. The structures of the synthesized compounds were generated and minimized using tripos force fields. All the other default parameters were used except the factor was the threshold was set to 0.6 when the protomol was generated. The highest-scored conformation based on the Surflex-Dock scoring functions, was selected as the final bioactive conformation.

The MD simulations were performed using AMBER 12 software package [26,27] according to our previously published protocol [28]. The missing residues, which were not solved in the crystal structures, were modeled using the loop building routine in Modeler [29]. Geometry optimization and the electrostatic potential calculations for gefitinib, **12c**, **12e**, and **7a** were carried out at the HF/6-31G* level of the Gaussian03 suite [30]. The atomic partial charge was obtained by using the restrained electrostatic potential (RESP) fitting technique [31] implemented in AmberTools [32]. The force field parameters for gefitinib, **12c**, **12e**, and **7a** were generated by the general amber force field (GAFF) [33] using the Antechamber program. The AMBER 99SB force field [34] was used to simulate the protein structure and the ionization state of amino acid residues were set according to the standard protocol. The model was neutralized by adding suitable counterions and were solvated in a truncated octahedron box of TIP3P [35] water molecules with a margin distance of 12 Å. The fully solvated and neutralized system was subjected to energy minimization. Following minimization, the system was gradually heated from 0 to 300 K in 50 ps using a Langevin thermostat with a coupling coefficient of 1.0/ps with a force constant 2.0 kcal mol^{-1} $Å^{-2}$ on the complex. And then 50 ps of density equilibration with a force constant 2.0 kcal mol^{-1} $Å^{-2}$ on the complex were performed. Subsequently the systems were again equilibrated for 500 ps by releasing all the restrains. Finally, the 20 ns MD production was performed at 300 K with 1.0 atm pressure. During the MD simulations, the long-range Coulombic interactions were handled using the particle mesh Ewald (PME) method [36]. The cutoff distance for the long-range vdW energy term was set at 10.0 Å. Periodic boundary conditions were applied to avoid edge effects in all calculations. The SHAKE algorithm [37] was employed on all atoms covalently bond to hydrogen atoms, allowing for an integration time step of 2 fs. Coordinate trajectories were recorded every 10 ps throughout all equilibration and production runs. The binding free energies (ΔG_{bind}) were calculated by using MM-GBSA [38] procedure in AMBER12. Average 1000 snapshots were extracted from the last 10 ns MD trajectory for the calculations, and only 10 snapshots evenly extracted from the last 10 ns MD trajectory were used to calculate the entropic contribution.

Acknowledgments

This work was supported by grants from National Science Foundation of China (No. 815732630 and 81202413) and Guangdong Natural Science Foundation (No. 2015A030313285). The calculations of the ligands were performed in the China ScGrid of Supercomputing Center of Chinese Academy of Science.

Appendix A. Supplementary data

Supplementary data related to this article can be found at http://dx.doi.org/10.1016/j.ejmech.2016.04.026.

References

[1] J. Mendelsohn, J. Baselga, The EGF receptor family as targets for cancer therapy, Oncogene 19 (2000) 6550–6565.
[2] F. Ciardiello, G. Tortora, EGFR antagonists in cancer treatment, N. Engl. J. Med. 358 (2008) 1160–1174.
[3] A. Harandi, A.S. Zaidi, A.M. Stocker, D.A. Laber, Clinical efficacy and toxicity of anti-EGFR therapy in common cancers, J. Oncol. 2009 (2009) 1–14.
[4] A. Gschwind, O.M. Fischer, A. Ullrich, The discovery of receptor tyrosine kinases: targets for cancer therapy, Nat. Rev. Cancer 4 (2004) 361–370.
[5] C. Carmi, A. Cavazzoni, S. Vezzosi, F. Bordi, F. Vacondio, C. Silva, S. Rivara, A. Lodola, R.R. Alfieri, S. La Monica, M. Galetti, A. Ardizzoni, P.G. Petronini, M. Mor, Novel irreversible epidermal growth factor receptor inhibitors by chemical modulation of the cysteine-trap portion, J. Med. Chem. 53 (2010) 2038–2050.
[6] K. Singh, P. Sharma, A. Kumar, A. Chaudhary, R. Roy, 4-Aminoquinazoline analogs: a novel class of anticancer agents, Mini Rev. Med. Chem. 13 (2013) 1177–1194.
[7] A.J. Barker, K.H. Gibson, W. Grundy, A.A. Godfrey, J.J. Barlow, M.P. Healy, J.R. Woodburn, S.E. Ashton, B.J. Curry, L. Scarlett, Studies leading to the identification of ZD1839 (Iressa™): an orally active, selective epidermal growth factor receptor tyrosine kinase inhibitor targeted to the treatment of cancer, Bioorg. Med. Chem. Lett. 11 (2001) 1911–1914.
[8] A.E. Wakeling, S.P. Guy, J.R. Woodburn, S.E. Ashton, B.J. Curry, A.J. Barker, K.H. Gibson, ZD1839 (Iressa) an orally active inhibitor of epidermal growth factor signaling with potential for cancer therapy, Cancer Res. 62 (2002) 5749–5754.
[9] E.R. Wood, A.T. Truesdale, O.B. McDonald, D. Yuan, A. Hassell, S.H. Dickerson, B. Ellis, C. Pennisi, E. Horne, K. Lackey, A unique structure for epidermal growth factor receptor bound to GW572016 (Lapatinib) relationships among protein conformation, inhibitor off-rate, and receptor activity in tumor cells, Cancer Res. 64 (2004) 6652–6659.
[10] K.N. Ganjoo, H. Wakelee, Review of erlotinib in the treatment of advanced non-small cell lung cancer, Biol. Targets Ther. 1 (2007) 335–346.
[11] Lee F. Allen, Irene A. Eiseman, David W. Fry, Peter F. Lenehan, CI-1033, an irreversible pan-erbB receptor inhibitor and its potential application for the treatment of breast Cancer, Semin. Oncol. 30 (2003) 65–78.
[12] E. Calvo, A.W. Tolcher, L.A. Hammond, A. Patnaik, J.S. de Bono, I.A. Eiseman, S.C. Olson, P.F. Lenehan, H. McCreery, P. LoRusso, Administration of CI-1033, an irreversible Pan-erbB tyrosine kinase inhibitor, is feasible on a 7-day on, 7-day off schedule a phase I pharmacokinetic and food effect study, Clin. Cancer Res. 10 (2004) 7112–7120.
[13] A. Gangjee, A. Vasudevan, S.F. Queener, R.L. Kisliuk, 6-substituted 2, 4-damino-5-methyl-pyri- do [2,3-d] pyrimidines as inhibitors of dihydrofolate reductases from Pneumocystis carinii and Toxoplasma gondii and as antitumor agents, J. Med. Chem. 38 (1995) 1778–1785.
[14] G.W. Rewcastle, B.D. Palmer, A.M. Thompson, A.J. Bridges, D.R. Cody, H. Zhou, D.W. Fry, A. McMichael, W.A. Denny, Tyrosine kinase inhibitors. 10. Isomeric 4-[(3-bromophenyl) amino] pyrido [d]-pyrimidines are potent ATP binding site inhibitors of the tyrosine kinase function of the epidermal growth factor

receptor, J. Med. Chem. 39 (1996) 1823–1835.
[15] D. Zhang, J. Ai, Z. Liang, C. Li, X. Peng, Y. Ji, H. Jiang, M. Geng, C. Luo, H. Liu, Discovery of novel 2-aminopyridine-3-carboxamides as c-Met kinase inhibitors, Bioorg. Med. Chem. 20 (2012) 5169–5180.
[16] W.M. Chen, S.H. Wan, New straightforward synthesis of 2-amino-6-methyl-5-(pyridin-4-ylsulfa- nyl)-3 H-quinazolin-4-one, Synth. Commun. 37 (2007) 53–61.
[17] M. Campiglio, A. Locatelli, C. Olgiati, N. Normanno, G. Somenzi, L. Viganò, M. Fumagalli, S. Ménard, L. Gianni, Inhibition of proliferation and induction of apoptosis in breast cancer cells by the epidermal growth factor receptor (EGFR) tyrosine kinase inhibitor ZD1839 ('Iressa') is independent of EGFR expression level, J. Cell. Physiol. 198 (2004) 259–268.
[18] G.E. Konecny, M.D. Pegram, N. Venkatesan, R. Finn, G. Yang, M. Rahmeh, M. Untch, D.W. Rusnak, G. Spehar, R.J. Mullin, Activity of the dual kinase inhibitor lapatinib (GW572016) against HER-2-overexpressing and trastuzumab-treated breast cancer cells, Cancer Res. 66 (2006) 1630–1639.
[19] F.M. Sirotnak, M.F. Zakowski, V.A. Miller, H.I. Scher, M.G. Kris, Efficacy of cytotoxic agents against human tumor xenografts is markedly enhanced by coadministration of ZD1839 (Iressa), an inhibitor of EGFR tyrosine kinase, Clin. Cancer Res. 6 (2000) 4885–4892.
[20] P. Warnault, A. Yasri, M. Coisy-Quivy, G. Cheve, C. Bories, B. Fauvel, R. Benhida, Recent advances in drug design of epidermal growth factor receptor inhibitors, Curr. Med. Chem. 20 (2013) 2043–2067.
[21] Y. Yang, Y. Shen, H. Liu, X. Yao, Molecular dynamics simulation and free energy calculation studies of the binding mechanism of allosteric inhibitors with p38α MAP kinase, J. Chem. Inf. Model. 51 (2011) 3235–3246.
[22] Burns Christopher john, B.U. Xianyong, Wilks Andrew Frederick, Protein kinase inhibitors, PCT Int. Appl. WO 03/099796, Cytopia Pty.Ltd, 2003.
[23] Sybyl 7.3, T.I., 1699 South Hanley Rd, St. Louis, MI 63144, USA.
[24] X. Wu, S. Wan, Z. Li, L. Yang, J. Zhang, S. Wu, 3D-QSAR study on 2, 3-dihydroimidazo [4, 5]-pyridin-2-one derivatives with a meta substitution pattern as $V600E^{BRAF}$ inhibitors, Med. Chem. Res. 23 (2014) 587–602.
[25] http://www.rcsb.org/pdb/explore/explore.do?structureId=4WKQ.
[26] D.A. Case, T.A. Darden, T.E. Cheatham III, C.L. Simmerling, J. Wang, R.E. Duke, R. Luo, R.C. Walker, W. Zhang, K.M. Merz, B. Roberts, S. Hayik, A. Roitberg, G. Seabra, J. Swails, A.W. Goetz, I. Kolossváry, K.F. Wong, F. Paesani, J. Vanicek, R.M. Wolf, J. Liu, X. Wu, S.R. Brozell, T. Steinbrecher, H. Gohlke, Q. Cai, X. Ye, J. Wang, M.J. Hsieh, G. Cui, D.R. Roe, D.H. Mathews, M.G. Seetin, R. Salomon-Ferrer, C. Sagui, V. Babin, T. Luchko, S. Gusarov, A. Kovalenko, P.A. Kollman, AMBER 12, University of California, San Francisco, 2012.
[27] R. Salomon-Ferrer, A.W. Götz, D. Poole, S. Le Grand, R.C. Walker, Routine microsecond molecular dynamics simulations with AMBER on GPUs. 2. Explicit solvent particle mesh Ewald, J. Chem. Theory Comput. 9 (2013) 3878–3888.
[28] X. Wu, S. Wan, G. Wang, H. Jin, Z. Li, Y. Tian, Z. Zhu, J. Zhang, Molecular dynamics simulation and free energy calculation studies of kinase inhibitors binding to active and inactive conformations of VEGFR-2, J. Mol. Graph. Model. 56 (2015) 103–112.
[29] K. Arnold, L. Bordoli, J. Kopp, T. Schwede, The SWISS-MODEL workspace: a web-based environment for protein structure homology modelling, Bioinformatics 22 (2006) 195–201.
[30] M. Frisch, G. Trucks, H. Schlegel, G. Scuseria, M. Robb, J. Cheeseman, J. Montgomery Jr., T. Vreven, K. Kudin, J. Burant, Gaussian 03, Gaussian, Inc., Wallingford, CT, 2004.
[31] C.I. Bayly, P. Cieplak, W. Cornell, P.A. Kollman, A well-behaved electrostatic potential based method using charge restraints for deriving atomic charges: the RESP model, J. Phys. Chem. 97 (1993) 10269–10280.
[32] J. Wang, W. Wang, P.A. Kollman, D.A. Case, Automatic atom type and bond type perception in molecular mechanical calculations, J. Mol. Graph. Model. 25 (2006) 247–260.
[33] J. Wang, R.M. Wolf, J.W. Caldwell, P.A. Kollman, D.A. Case, Development and testing of a general amber force field, J. Comput. Chem. 25 (2004) 1157–1174.
[34] V. Hornak, R. Abel, A. Okur, B. Strockbine, A. Roitberg, C. Simmerling, Comparison of multiple Amber force fields and development of improved protein backbone parameters, Proteins Struct. Funct. Bioinform. 65 (2006) 712–725.
[35] W.L. Jorgensen, J. Chandrasekhar, J.D. Madura, R.W. Impey, M.L. Klein, Comparison of simple potential functions for simulating liquid water, J. Chem. Phys. 79 (1983) 926–935.
[36] T. Darden, D. York, L. Pedersen, Particle mesh Ewald: an N log (N) method for Ewald sums in large systems, J. Chem. Phys. 98 (1993) 10089–10092.
[37] J.P. Ryckaert, G. Ciccotti, H.J. Berendsen, Numerical integration of the cartesian equations of motion of a system with constraints: molecular dynamics of n-alkanes, J. Comput. Phys. 23 (1977) 327–341.
[38] P.A. Kollman, I. Massova, C. Reyes, B. Kuhn, S. Huo, L. Chong, M. Lee, T. Lee, Y. Duan, W. Wang, Calculating structures and free energies of complex molecules: combining molecular mechanics and continuum models, Acc. Chem. Res. 33 (2000) 889–897.